Development of Observation-based Parameterizations of Standard Deviations of Wind Velocity Fluctuations over an Indian Region

Piyush Srivastava*, Maithili Sharan
Centre for Atmospheric Sciences,
Indian Institute of Technology Delhi, India

Manoj Kumar
School of Natural Resource Management
Center for Environmental Sciences
Central University Jharkhand, India

***Corresponding Author:**
Dr. Piyush Srivastava
Centre for Atmospheric Sciences,
Indian Institute of Technology Delhi, India
Current affiliation:
School of Earth and Environment
University of Leeds, United Kingdom
Email: piyoosh.iitr@gmail.com

Abstract

The present study utilizes the turbulence observations over an Indian region, Ranchi, to study the diurnal and seasonal characteristics of mean and turbulent parameters in the atmospheric surface layer under different wind speed and stability regimes. Data for the year 2009 are chosen to compute mean and turbulent statistics using the eddy correlation technique and are studied within the framework of Monin–Obukhov similarity theory. The analysis of the observational behavior of the standard deviation of wind velocity fluctuations (σ_i, $i = u, v, w$) normalized by friction velocity (u_*) suggests that these parameters remain independent of stability of layer in near-neutral to moderately stable/unstable conditions. However, they are observed to increase following the classical 1/3 power law with increasing stability/instability in moderate to strong stable/unstable conditions. Further, an attempt has been made to develop possible parameterizations of these coefficients in terms of Monin-Obukhov stability parameter in low and moderate to strong wind regimes for four different seasons. The proposed observation-based functional forms the σ_i as functions of the stability exhibit different behaviours depending on the optimal values of unknown coefficients obtained for different seasons. However, within the limit of the uncertainty in the observed input parameters, the values of the season-dependent set of coefficients do not affect the overall statistical agreement between predicted and observed values of the normalized standard deviation of wind velocity fluctuations.

Keywords: Atmospheric Surface Layer, Surface Fluxes, Mean and Turbulent Characteristics, Monin-Obukhov Similarity theory, Parameterization

1 Introduction

The turbulent structure of the atmospheric boundary layer is poorly described in low wind conditions. The complexity of the boundary layer grows with the weakening of the winds and the degree of atmospheric stability (Mahrt, 1998; Mahrt, 2008; Luhar et al., 2009). The scarcity of data in low wind convective as well as very stable conditions over the tropical region has resulted in a limited understanding of turbulence structure in such types of atmospheric conditions (Gopalakrishnan et al., 1998; Aditi and Sharan, 2007). The limited knowledge of the boundary layer characteristics and their representation in numerical models is a major contributing factor for relatively poor performance of almost all dispersion models under low wind and very stable/unstable conditions (Sharan et al., 1996; Kumar and Sharan, 2010; Qian and Venkatram, 2011). The diffusion of a pollutant released from various emission sources is irregular and indefinite in weak and variable wind conditions (Sharan et al., 2012). Various studies reported in the literature (Sharan et al., 1995; Yadav and Sharan, 1996; Anfossi et al., 2006; Luhar, 2011) suggest that the operational dispersion models fail to predict the observed concentrations under low wind conditions due to inadequate understanding of turbulence and dispersion characteristics in these conditions. The dispersion of pollutants in the atmosphere is influenced by the standard deviation of wind velocity fluctuations (σ_u, σ_v and σ_w). These parameters provide useful information regarding the turbulent state of the atmospheric and are used as important inputs implicitly as well as explicitly to almost all dispersion models (Hanna et al., 1982; Sharan et al., 1999; Holmas and Morawska, 2006; Luhar, 2010; Kumar and Sharan, 2010; Kumar and Goyal, 2014; Pandey and Sharan, 2017). Thus, an accurate prescription of these parameters is required as input in the dispersion models for improved estimation of the concentration of air pollutants released from various sources. Turbulence measurements are seldom collected on a routine basis making it essential to parameterize these quantities with the help of field data under different stability and wind speed regimes over different topographical conditions that can be directly incorporated into dispersion models at different scales. According to the Monin-Obukhov similarity theory (MOST, Monin and Obukhov, 1954) σ_u, σ_v and σ_w when normalized by friction velocity u_*, are universal functions of Monin-Obukhov stability parameter ζ (Arya, 1988). Note that whether or not the MOST, within the existing framework, is valid in the very stable conditions (Mahrt, 1998; Klipp and Mahrt, 2004; Cheng and Brutsaert, 2005; Grachev et al., 2007; Mahrt, 2008; Kumar and Sharan, 2012; Mahrt, 2014) and very unstable conditions (Rao and Narashima, 2006; Srivastava and Sharan, 2015) is still an open question. However, in spite of the limitations, MOST is being extensively used to parameterize surface flux in almost all numerical models of the atmosphere (Skamarock et al., 2008; Giorgi et al., 2012; Gopalakrishnan et al. 2013; Jun Zhang et al., 2015), forward dispersion models (Kumar and Sharan, 2010) and inverse modeling of source identification (Kumar et al., 2015). Simultaneously, the applicability of MOST in very stable/unstable conditions is being evaluated with measurements of turbulence in the atmospheric surface layer over different topographical conditions.

Based on theoretical concepts as well as analysis of turbulence data, a number of expressions for the turbulence statistics, in terms of the stability parameter and wind speed in the atmospheric surface layer, have been proposed in the literature (Panofsky et al., 1977; Kaimal and Finnigan, 1994; Rannik ,1998; Sharan et al., 1999; Pahlow et al., 2001; Martin et al., 2009; Franceschi et al. 2009; Wood et al. 2010; Trini Castelli and Falabino, 2013; Nadeau et al., 2013; Grachev et al., 2013; Trini Castelli et al., 2014; Grachev et al., 2018). However, the studies are limited to the mid-latitudes, and very few studies have been carried out over the Indian region (Ramachandranan et al., 1994; Agarwal et al., 1995; Krishnan and Kunhikrishnan, 2002; Ramana et al., 2003). The results presented in these studies are valid in a narrow range of wind speed and stability regimes. Ramachandranan et al. (1994) have analyzed the nature of normalized standard deviations of wind velocity components over a coastal site in daytime conditions only. Agarwal et al. (1995) analyzed a very limited dataset collected from a micrometeorological tower installed at IIT Delhi (India) campus using a sonic anemometer at the height of 4 m. Although the dataset covers a wide range of stability and wind, the number of data points in each of wind and stability regimes were very less to derive any definite conclusion regarding the functional behavior of normalized standard deviations of wind velocity components. Further, due to the empirical nature of these expressions, it is of interest to investigate the applicability of these parameterizations under different atmospheric and topographic conditions (Trini Castelli and Falabino, 2013; Trini Castelli et al., 2014). Various studies have pointed out that turbulent strength relationships depend on the underlying surface cover and local atmospheric conditions of the measurement site (Prasad et al., 2018). One can also expect the variation in the values of these parameters in different seasons and thus, it does not appear legitimate to apply same parameterization in different seasons without proper validation. In the present study, we have made an attempt to validate and improve the relationships of standard deviations of wind velocity components utilizing one-year-long continuous turbulence measurements in a wide range of wind and stability regimes. The objectives of the present study are to (1) study the seasonal and diurnal variation of surface layer parameters and turbulent fluxes, (2) develop observation-based parameterizations of standard deviations of wind velocity fluctuations under different stability and wind speed regimes in different seasons and (3) evaluate the empirical expressions proposed earlier in order to assess the extent of their applicability.

2 Site Description and Data Analysis

The observation data used in the present study is obtained from a CSAT3 sonic anemometer mounted on a 32 m tower installed at Birla Institute of Technology Mesra, Ranchi (23.412° N, 85.440° E), India (Tyagi and Satyanarayana 2013; Dwivedi et al., 2014). The description of the site, dataset and data quality control method parallels that of Srivastava and Sharan (2015) and Srivastava and Sharan (2019). A fast response sensor was installed at 10-m height that measures the three components of wind and temperature at 10 Hz frequency. The approach of Vickers and Mahrt (Vickers and Mahrt, 1997) is adapted for removing the spikes present in the dataset. After the quality check, data were rotated into a streamline coordinate system using 2-D rotation technique.

From the turbulence measurements, frictional velocity u_* and temperature scale θ_* are calculated from the expressions

$$u_* = \left[\left(\overline{u'w'} \right)^2 + \left(\overline{v'w'} \right)^2 \right]^{1/4} \tag{1}$$

and

$$\theta_* = -\frac{\overline{w'\theta_v'}}{u_*}, \tag{2}$$

in which u', v' and w' are, respectively, the fluctuations in longitudinal, lateral, and vertical wind components and $\overline{\theta}_v$ is the mean virtual potential temperature at height z.

The sensible heat flux (H) is calculated using an expression

$$H = -\rho C_p u_* \theta_*, \tag{3}$$

in which ρ is the density of the dry air and C_p is specific heat capacity at constant pressure.

The stability parameter ζ is calculated from the expression

$$\zeta = z/L = -\frac{kzg\left(\overline{w'\theta_v'}\right)}{\overline{\theta}_v u_*^3}, \tag{4}$$

where g is acceleration due to gravity. The value of sonic temperature θ_s is very close to the virtual potential temperature $\theta_v = \theta(1 + 0.61q)$, in which q is the specific humidity. Thus, $\theta_v = \theta_s$ is taken for computing the value of ζ from turbulence measurements. Note that the sonic temperature can be directly used to estimate the buoyancy flux, and thus the stability parameter ζ (Eq. 4). The sonic temperature has a water vapor contribution, which needs to be corrected for computing the correct value of the heat flux from Eq. (3). However, due to unavailability of humidity measurements, this correction has not been applied here, and heat flux is estimated directly using the fluctuations in the sonic temperature.The whole dataset of the year 2009 is divided according to four seasons, (i) Pre-monsoon (March, April and May), (ii) Monsoon (June, July, August, September), (iii) Post-monsoon (October, November and December), and (iv) Winter (January and February). To minimize the effect of the rainfall on the turbulence measurements, the data points corresponding to the one hour before and after rainfall are also excluded. In each of the season, the dataset is further divided based on the wind speed and the stability regimes. Since most of the data points corresponding to the range $U > 2$ m/s are falling in the range $2 < U \leq 6$ m/s and only ~2% data belongs to the range $U \geq 6$ m/s, we refer all the data points corresponding to $U > 2$ m/s to moderate wind condition. The quantitative description of data is given in Figure 1.

Depending upon the average time of sunrise and sunset in each of the months, a transition regime is identified and corresponding data are excluded for the analysis of the turbulence parameter. The rest of the data are further divided into two categories, namely, 'daytime data' and 'nighttime data'. The atmosphere is observed to be significantly unstable during Pre-monsoon season as compared to the other seasons. Moderate winds (U > 2 m/s) are relatively more associated with the unstable condition as compared to low wind conditions (U < 2 m/s) in each of the seasons. However, the wind is generally observed to be low in stable conditions (~80%). It is observed that during the nighttime, for a significant amount of data, ζ attains a negative value, which corresponds to unstable conditions. The data points showing nighttime unstable and daytime stable are excluded from the regression analysis. However, from the study point of view, these data points are analyzed separately (Table -1).

3 Observational Behavior of Surface Layer Parameters in Different Seasons

Time averages of sonic temperature (Kelvin) for different seasons with respect to Indian Standard Time (IST) are shown in Figure 2. In each of the panels of Figure 2, the vertical error bars represent one standard deviation from the mean value of each parameter at that particular time. The temperature attains the minimum value just before the sunrise (0500-0600 IST) and a maximum value at around 1300-1400 IST, which is consistent with the physical characteristics of the temperature in each of the seasons. The average maximum (minimum) temperatures are found to be 306.13 K (295.59 K), 305.0 K (299.52 K), 298.05 K (288.28 K), and 299.07 K (286.61 K) in Pre-monsoon, Monsoon, Post-monsoon and Winter seasons respectively. The maximum diurnal variability in temperature is observed in winter season while the minimum variability is observed during the monsoon season. The minimum variability in the diurnal temperature during monsoon season can be attributed to the associated rainfall during this season.

The wind speed at 10 m height over Ranchi is shown in Figure 3 for different seasons. The low wind conditions prevail almost all over the year. The moderate wind conditions are predominately observed in Pre-monsoon season as compared to the other seasons. The diurnal variation of U shows that the wind remains low during nighttime and moderate to high during the daytime. However, there are a large number of individual hours for which wind speed is found to fall in the range $5 < U < 9$ m/s.

The sensible heat flux (H) (W/m^2) estimated using the eddy correlation technique (Eq. 3) in different seasons are plotted with respect to IST in Figures 4(a, b, c, d). The error bars in figure indicate one deviation from the mean value of H. The temporal evolution of H appears to be similar in different seasons. However, appreciable seasonal differences in the magnitude of H are observed. The average maximum values of daytime heat flux in convective condition are found to be 214.30 (+/-78.0) W/m^2, 105.47 (+/-64.64) W/m^2, 142.64 (+/-47.64) W/m^2, and 188.46 (+/-54.06) W/m^2 in Pre-monsoon, Monsoon, Post-monsoon and Winter season respectively. The magnitude of H is observed to be the highest during Pre-monsoon season and the lowest in Monsoon season. However, the magnitude of H is found to be comparable during Post-monsoon and winter seasons. One of the possible reasons for the low values of H in Monsoon season may be intermittent rainfall during the entire season and the presence of clouds over the region.

The Obukhov length is generally used to classify different stability regimes in air pollution as well as other meteorological applications. In order to study the general characteristics of the observational site, the frequency of occurrence of the stability parameter computed using Eq. (4) in different seasons is shown in Figure 5. The data points obtained in daytime unstable conditions fall in the range $-100 < \zeta < 0$, while nighttime stable conditions correspond to the range of value stability parameter lying in the range $0 < \zeta < 100$. It is evident from the Figure 5 that the dataset covers a wide range of stability conditions in each of the seasons with a bi-modal distribution having one peak in the stable regime and another peak in the unstable regime while the bins are logarithmically spaced. Moderate to high stability/instability is mostly associated with the low wind conditions and due to the high frequency of occurrence of low wind conditions in both stable and unstable conditions, near-neutral to moderately stable/unstable conditions are relatively less as compare to moderate to highly stable/unstable conditions in each season.

A very interesting feature of nighttime unstable and daytime stable conditions (Table 1) is found to occur. However, a closer analysis of the data reveals that approximately 95% cases of nighttime unstable conditions are associated with low wind conditions. Since in the present study, the data points corresponding to the transition regime have been excluded, the phenomenon of the nighttime unstable condition does not appear to be associated with the range of split of Day and Night period (Trini Castelli and Falabino, 2013). The analysis of data shows that in such cases, both the values of friction velocity and heat flux appear to be very small, which can result in a change of sign of the Obukhov length. These findings are in good agreement with the studies reported in the literature (Trini Castelli and Falabino, 2013; Trini Castelli et al., 2014) and further suggest the use of ζ based classification of different stability regimes in air-pollution modeling with caution particularly under low wind conditions.

4 Standard Deviation of Wind Velocity Fluctuations

4.1 Observational Behaviour

Figure 6 shows the normalized standard deviations of the vertical velocity component σ_w/u_* versus the local Monin-Obukhov stability parameter ζ in the logarithmic axis for turbulence data over Ranchi from Pre-monsoon, monsoon, Post-monsoon and Winter seasons under stable conditions (i.e., $\zeta > 0$). The data are divided into low wind and moderate wind regimes with left panels (Fig. 6a, c, e, g) presenting moderate wind conditions (U > 2 m/s) and right panels (Fig. 6b, d, f, h) representing low wind conditions (U < 2 m/s). The similar plots of the normalized standard deviations of the longitudinal and lateral velocity components are shown in figure 7 and 8. Figure 7 suggests that in near-neutral conditions, the values of σ_w/u_* do not vary significantly and appear to be independent of stability with the maximum (minimum) value 1.35(1.11) and the values are observed to increase with increasing stability in moderate to strong stable conditions in both the wind regimes. However, there is a large scatter in the values of σ_w/u_* in low wind conditions as compared to moderate wind conditions. The near-neutral values of σ_w/u_* in Pre-monsoon and Post-monsoon seasons are observed to be comparable to the values reported over the tropics as well as mid-latitudes and it is found to be consistent with the studies reported in the literature over Indian region in Monsoon and Winter seasons. Similar results are obtained for normalized standard deviations of the longitudinal (σ_u/u_*) and lateral velocity (σ_v/u_*) components (Fig. 7 and 8) and data from different seasons appears to follow a universal pattern similar to the nature of normalized component of vertical velocity component. In the near-neutral conditions, the values of σ_i/u_*, i = u, v are found to be 2.54(2.30) and 2.45(2.01) respectively.

Similar to the stable conditions, the plots for the normalized standard deviations of the vertical, longitudinal and lateral velocity components for unstable stratification are shown in figures 9, 10 and 11 respectively. A good correlation between σ_i/u_* and $-\zeta$ is observed under both the wind regimes in all the four seasons for all three components. This is in agreement with the classical 1/3 power law (Panofsky and Dutton, 1984; Moraes et al., 2005; Martin et al., 2009; Trini Castelli and Falabino, 2013). As compared to stable conditions, there is relatively less scatter in the values of σ_i/u_* under the unstable conditions in both the wind regimes. Weak and intermittent turbulence might be one of the reasons for large scatter observed in the stable conditions as compared to the unstable conditions. The scatter is found to increase with increasing instability. However, all three components appear to follow a classical '1/3 power law' with a better correlation in moderate wind unstable conditions as compared to low wind conditions. The normalized vertical component of velocity shows the best correlation with stability in moderate wind unstable conditions, which is consistent with the study of Panofsky and Dutton (1984).

Pahlow et al. (2001) analyzed the turbulence measurements from several field experiments to understand the turbulence characteristics under stable conditions. They found that the value of σ_i/u_* remains constant up to $\zeta \approx 0.1$. These constants are found to be equal to 2.3, 2 and 1.1 respectively for σ_u/u_*, σ_v/u_* and σ_w/u_*. However, for very stable conditions, σ_i/u_* increases strongly with increasing stability beyond $\zeta \approx 0.1$. Note that Pahlow et al. (2001) have not studied the turbulence characteristics separately for weak and strong wind conditions and in the present study, we have observed significant differences in the near-neutral values of these parameters depending upon the wind speed regime.

Based on the analysis of the data at 10 m height over a coastal equatorial urban location during south-west Monsoon season, Yusup et al. (2008) observed that the parameters σ_u/u_* and σ_v/u_* increase linearly with increasing values of ζ under stable conditions. However, no systematic dependence was observed in the case of σ_w/u_* under stable conditions. Trini Castelli and Falabino (2013) have analyzed the nature of standard deviations of the wind velocity fluctuations in the surface layer based on the extensive analysis of the turbulence data obtained over three different sites and proposed empirical curves for low winds under both stable and unstable conditions. They further investigated the dependency of the neutral values of σ_u/u_*, σ_v/u_* and σ_w/u_* on the wind speed to find a general relationship for these parameters as a function of stability parameter, those can be used in dispersion models irrespective of wind speed regime. The higher values of near-neutral values of these parameters under low wind conditions are found to occur as compared to those observed under moderate wind conditions, which is consistent with the results obtained in the present study.

From the analysis of measurements over a forest region in southern Finland, Rannik (1998) found that normalized variances of *u*, *v* and *w* components remains fairly constant in the near-neutral stability. The corresponding average values are reported to be 2.25, 1.82, and 1.33 respectively for *u*, *v* and *w* components. The near-neutral value of the vertical component is in agreement with that found in the present study. However, the values of horizontal and lateral components are relatively smaller than those found in the present dataset. Rannik (1998) reported that under stable stratification σ_w/u_* increases significantly for $\zeta > 0.1$. The similar increase has also been observed for *u* and *v* components under stable conditions. Further, under unstable stratification, all three components were found to follow 1/3 power law. These findings are consistent with those reported in the present study.

Babić et al. (2016a) analyzed multi-level turbulence observations over a heterogeneous surface under stable conditions. They evaluated the normalized standard deviations by utilizing the functional form similar to the present study but the exponent *c* (Eq. 5) has been treated as a free variable. They reported that the values of σ_i/u_*, $i = u, v, w$ depend on the measurement heights with the smallest values, in general, correspond to the lowest level of measurements. The values of σ_i/u_* reported by Babić et al. (2016a) are in general smaller than those obtained in the present study and reported over flat terrain (Kaimal and Finnigan, 1994). However, those values are in good agreement to those found over 'physically' similar type of terrain (Moraes et al., 2005; Wood et al., 2010).

Nadeau et al. (2013) analyzed turbulence measurements over a steep mountain slope and found that near-neutral values of σ_i/u_*, i = u, v, w as 2.85, 2.24 and 0.98 respectively. Similar to the present study, they have found that 1/3 power law works reasonably well and derived the empirical formulations of σ_i/u_* under both stable and unstable conditions. However, Nadeau et al. (2013) reported better statistical performance of the derived relationships for stable conditions while the present study suggests that the proposed relationships perform relatively better for moderate wind unstable conditions. Similar to the present study, Nadeau et al. (2013) found that the vertical component is relatively better correlated with the stability parameter as compared to the lateral and horizontal components.

Babić et al. (2016b) have investigated the impact of the non-stationarity on the unknown coefficients appearing in the functional form of σ_i/u_* (Eq. 5) over complex terrain. They argued that the differences in the near-neutral values of complex and flat terrain might be partially associated with the non-stationarity. Stiperski and Rotach (2016) have discussed the effects of data quality and post-processing options on the derived functional forms of σ_i/u_*. Similar to the present study. Babić et al. (2016b) have also utilized 1/3 power-law dependent form of σ_i/u_* for the analysis.

Wood et al. (2010) have analyzed the nature of σ_i/u_* with stability over an urban area using turbulence observations taken at 190.3 m height. They found the near-neutral values of σ_i/u_*, i = u, v, w as 2.3, 1.85 and 1.35 respectively. The observed variation of σ_i/u_* is found to follow 1/3 power law under unstable conditions, which is consistent with the present study. However, under stable conditions, the exponent c (Eq. 5) is reported to have a smaller value than that found in the present. Similar to the present study, the scatter in the values of the normalized vertical component is reported to be relatively less as compared to the horizontal and vertical components suggesting that the vertical component is, in general, better correlated with the stability parameter as compared to the other two components of wind velocity.

Recently Grachev et al. (2018) have analyzed the nature of normalized standard deviation of wind velocity components over a coastal area using multilevel turbulence observations. They argue that these parameters, in general, follow the MOST for both sable and unstable conditions within the limit of possible uncertainty in the observations. The near-neutral values of σ_i / u_*, $i = u, v, w$ for their dataset are found to be equal to 2.39, 1.92 and 1.25 respectively. The near-neutral values of σ_u / u_* and σ_w / u_* are in good agreement with those found in the present study. However, the near-neutral value of the lateral velocity component found for the present data is relatively higher as compared to that reported by Grachev et al. (2018) over the coastal region. The analysis of Grachev et al. (2018) suggests that over a coastal area the observed values of σ_i / u_*, $i = u, v, w$ follow the Kansas-type functions (Kaimal and Finnigan, 1994).

Fig. (12) shows the comparison of functional relationships of $\sigma_{u,w} / u_*$ with respect to ζ derived from present data set in different seasons (solid lines with different colours) with those suggested by Kaimal and Finnigan (1994) (red dashed lines) under stable conditions. For weakly to moderately stable conditions $0 < \zeta < 0.1$, the proposed formulations of σ_u / u_* and σ_w / u_* are found to be in close agreement to the corresponding Kansas-type functions (Fig. 12). However, for $\zeta > 0.1$, there is a considerable difference in the functional behaviour of proposed formulations and Kansas-type functions. In the low-wind stable conditions, the proposed formulation of σ_u / u_* increases with respect to ζ with a relatively higher rate as compared to the Kansas-type functions. However, for the moderate wind stable conditions, Kansas-type functions fall within the variability of proposed formulations in different seasons (Fig. 12). In the case of the vertical velocity component, the Kansas-type functions show a relatively higher rate of increase as compared to that shown by proposed formulations in low wind stable conditions. For weakly to moderately unstable conditions $-0.1 < \zeta < 0$, the proposed formulations are in close agreement with the Kansas-type functions (Fig. 13). However, the Kansas-type functions are found to increase at a relatively higher rate for low wind conditions in moderately to strongly unstable conditions $\zeta < -0.1$ (Fig. 13) for both σ_u/u_* and σ_w/u_* expect for σ_u/u_* in moderate wind conditions.

Surface layer turbulence characteristics over an Indian region have been analyzed in few studies. For example, using data obtained at 5 m height, Kunhikrishnan (1990) reported the average values of σ_u/u_* and σ_v/u_* as 2.47 ± 0.22 and 1.97 ± 0.25 respectively, which are relatively lower compared to those obtained in the present study. Ramachandran et al. (1994) analyzed data at 5 m and 25 m height from southwest Monsoon and Northwest Monsoon seasons on the west coast of India under daytime convective conditions and found relatively lower values of σ_i/u_* as compared to those reported in the present study as well as suggested by Kunhikrishnan (1990). Agarwal et al. (1995) analyzed the data collected from a micrometeorological tower installed at IIT Delhi campus using a sonic anemometer at the height of 4 m. The study suggests that variances of longitudinal σ_u, lateral σ_v and vertical σ_w velocity fluctuations normalized by friction velocity do not have a significant variation for wind speeds greater than 1 m/s (Agarwal et al., 1995). The average values of the ratios σ_u/u_*, σ_v/u_* and σ_w/u_* were found to be equal to 2.08, 1.83 and 1.18 respectively, for daytime convective conditions, whereas the corresponding values for nighttime stable conditions were reported to be 1.90, 1.59 and 1.27 respectively. However, for mean wind speed less than 1 m/s these ratios were reported to be 2.47, 2.72, 1.55 for daytime unstable conditions and 4.44, 4.25, 1.79 for stable conditions. Note that the values obtained under unstable conditions are in good agreement with those found in the present study in both low and moderate wind conditions. However, the values of these parameters obtained under low wind stable conditions by Agarwal et al. (1995) are significantly larger than those found in the present study. Krishnan and Kunhikrishnan (2002) analyzed data from a tropical inland station Ahmedabad (India) and found the average values of σ_u/u_*, σ_v/u_* and σ_w/u_* equal to 2.32 ± 0.39, 2.29 ± 0.22, and 1.37 respectively in near-neutral conditions. They found no systematic dependence of the values of σ_u/u_* and σ_v/u_* on the values of ζ. However, the values of σ_w/u_* are found to increase with increasing stability and instability. Ramana et al. (2003) analyzed turbulence measurements at 10 m height over a tropical site Lucknow (India) in different seasons and pointed out that turbulence statistics are nearly independent of season. They have suggested that the value of σ_w/u_* increases with increasing instability and follows a 1/3 power law in free convective conditions and follow a linear profile under stable conditions in all the four seasons. The near-neutral value of σ_w/u_* was reported to be 1.05, 1.01, 0.94 and 1.0 during Winter, Pre-monsoon, monsoon and Post-monsoon seasons respectively. These values are relatively smaller than those observed in the present study in all the seasons. This might be partially attributed to distinguishing the whole data in two distinct wind speed regimes and frequency of occurrence of low wind conditions at present observation site. Further, the local atmospheric and topographical features appear to affect the near-neutral values of these parameters. Ramana et al. (2003) did not find any functional relationship between $\sigma_{u,v}/u_*$ and ζ. However, the values of these non-dimensional parameters are found to increase with increasing instability and stability. The average near-neutral values of σ_u/u_* and σ_v/u_* at 10 m level for all the seasons are reported to be 2.03 ± 0.36 and 2.19 ± 0.06 respectively.

4.2 Development of Empirical relationships

A nonlinear curve fitting is applied to the data to obtain normalized σ_i 's as functions of ζ. The functional form chosen for this purpose is similar to that reported in the literature (Moraes et al., 2005; Trini Castelli et al., 2014; Tyagi and Satyanarayana et al., 2013), i.e.,

$$\frac{\sigma_i}{u_*} = a\left[1 + b\left(\frac{z}{L}\right)\right]^c, \tag{5}$$

in which the constant *a*, *b* and *c* are determined for different stratification and seasonal conditions. In each of the figures (Figures 6-12), the solid lines show the best fit curve obtained using the least square technique. Note that in the neutral conditions, i.e., $\zeta \approx 0$ the value of $\sigma_i/u_* = a$, however, in the observational analysis the parameter *a* is calculated as the average value of σ_i/u_* in the stability range (-0.01, 0.01), *c* is fixed as 0.33 and the other coefficient *b* is left to vary independently and the best-fit values of the parameter *b* are obtained. Some of the researchers have suggested that the value of the parameter *c*, usually taken as equal to 0.33, might be an over prediction and the true value should be less than 0.33 (Yusup et al., 2008; Agarwal et al., 1995). However, in the present study, we observe that the value of *c* does not differ significantly from 0.33 which is in good agreement with the earlier studies (Trini Catelli et al., 2014; Moraes et al., 2005; Martin et al., 2009). The estimated values of the parameters *a* and *b* are shown in Table 2. The values of *a* for the normalized horizontal and lateral components of wind velocity standard deviations (near-neutral values of σ_i/u_*, $i = u, v$) are observed to be higher in the low wind as compared to moderate wind condition under both stable and unstable conditions in all seasons. However, in Post monsoon season the larger values are observed in moderate wind conditions. The near-neutral values of normalized vertical wind standard deviation are observed to be smaller in low wind conditions as compared to moderate wind conditions in the stable as well as unstable conditions. Recently, Tyagi and Satyanarayana (2013) have utilized the data obtained from the same site taken in the present study during the Pre-monsoon season of the years 2008-2010 to analyze the difference in the boundary layer characteristics during a thunderstorm

(TD) and non-thunderstorm (NTD) days. They have also observed the 1/3 power-law dependence of the parameters σ_i/u_* on the stability parameter and proposed empirical expressions for σ_i/u_* under stable and unstable conditions for TD and NTD days. The unknown coefficients appearing in the empirical expressions in Pre-monsoon seasons, obtained in the present study, are relatively higher in magnitude to those obtained by Tyagi and Satyanarayana (2013) during NTD days in both low and moderate wind conditions. This may be attributed to the fact that in the present analysis, we have considered the low wind and moderate wind conditions separately for development of empirical formulations, while no such distinction is made by Tyagi and Satyanarayana (2013).

4.3 Applicability of the Proposed Expressions

Notice that the coefficients *a* and *b* appearing in the empirical expressions are found to vary in different seasons. However, it remains unclear whether the seasonal differences in the empirical expressions are statistically significant as compared to the uncertainty in the measurement of input parameters. Thus, in order to evaluate whether the coefficients from one season might be used in other seasons, we have calculated statistical metrics for different cases. For example, the expressions derived from data obtained during Pre-monsoon season are evaluated using observed values of $\sigma_i\ (i=u,v,w)$ u_* and ζ from 3 other seasons namely Post-monsoon, Monsoon, and Winter. For this purpose, the predicted values of σ_i are computed from the expression derived using data from Pre-monsoon seasons (referred to base season) and observed values of u_* and ζ from other seasons. The observed values of σ_i are computed from the turbulence measurements in the corresponding seasons and the predicted values are then compared to the observed values. The same procedure has been repeated by considering the base seasons as Post-monsoon, Monsoon and Winter. We have performed the statistical analysis, estimating the following metrics: fractional bias

(FB), normalized root mean square error ($NMSE$) and correlation coefficient (r) defined as (Chang and Hanna, 2004)

$$FB = 2\frac{\overline{O}-\overline{P}}{\overline{O}+\overline{P}} \tag{6}$$

$$NMSE = \frac{1}{n}\frac{\sqrt{\sum_{i=1}^{n}\left(O_i - P_i\right)}}{\overline{P}\,\overline{M}} \tag{7}$$

$$r = \frac{\sum_{i=1}^{n}\left(O_i - \overline{O}\right)\left(P_i - \overline{P}\right)}{\sqrt{\sum_{i=1}^{n}\left(O_i - \overline{O}\right)^2}\sqrt{\sum_{i=1}^{n}\left(P_i - \overline{P}\right)^2}} \tag{8}$$

in which 'O' stands for the observed, 'P' stands for the predicted, and symbol of over-bar shows the corresponding average value. Notice that the use of coefficients derived from one season in the other seasons, generally worsen the statistics (Tables 3 and 4). However, considering the errors involved in the turbulence measurements and input parameters, from the statistical point of view, the bias generated due to the use of a set of coefficients from one season in another season is not significant. Thus, although it appears that the empirical formulae are season-dependent, they are statistically similar and parameterizations developed using data from one season can be utilized in other seasons without introducing significant bias.

Notice that self-correlation occurs in the plots of σ_i/u_*, $i = u, v, w$ with respect to ζ because of the fact that friction velocity u_* appears in both the definitions of the dependent variable (σ_i/u_*, $i = u, v, w$) and independent variable (ζ). Grachev et al. (2013) have proposed a new approach to overcome the impact of self-correlation on such analysis. This approach is based on the fact that the combination of two Monin-Obukhov universal functions should be a universal function (Grachev et al., 2013; Babić et al., 2016a). Following the approach of Grachev et al. (2013), we have first estimated the values of

$\varphi_u/\varphi_w = \sigma_u/\sigma_w$ and $\varphi_v/\varphi_w = \sigma_v/\sigma_w$ from the observational data and potted them with respect to ζ for different seasons and wind and stability regimes. The corresponding ratios of universal functions derived from the present dataset are embedded in the scatter plots to analyse the influence of self-correlation. Fig. (14) shows the variation of σ_u/σ_w versus ζ for different seasons under stable conditions similar to Fig. (6). Similar to Fig. (6), large scatter in the values of σ_u/σ_w is observed in the low wind conditions (Fig. 14a, c, e, f) as compared to moderate wind conditions (Fig. 14b, d, g). However, the scatter of the data around the proposed formulations for different seasons does not change significantly (Fig. 6 and Fig. 14). This suggests that the power law dependence of proposed formulations is not likely due to self-correlation between dependent and independent variables. Similar behaviour is also observed for σ_v/σ_w (Fig. 15) under stable conditions. This nature appears to be consistent for unstable conditions also (Figs. 16, 17). We would like to point out that the observed values of σ_u/σ_w and σ_v/σ_w are found to increase with a relatively slow rate and even slightly decrease in some cases as compared to those found for σ_u/u_* and σ_v/u_*. Although the proposed formulations are able to capture the behaviour, this nature needs to be analyzed further.

5 Conclusions

Turbulence data over Ranchi (India) is utilized to analyze the mean and turbulence characteristics of the atmospheric surface layer. Data obtained from a sonic anemometer at 10 m height for the year 2009 is used to compute mean surface layer parameters such as wind speed and temperature, and turbulence parameters such as surface heat flux, friction velocity, Monin-Obukhov similarity parameter and standard deviations of wind velocity fluctuations in different seasons. Data are classified according to the four seasons and different wind speed and stability regimes.

The diurnal variation of wind speed is analyzed in different seasons, which suggests that the wind remains low during nighttime, follows a diurnal pattern reaching a maximum value during the early hours of the afternoon. A physically consistent diurnal behavior of 10 m air temperature is observed in each of the seasons with the maximum (minimum) variability (i.e., the difference between the average maximum and minimum temperature in a season) in the average temperature is found to occur in Winter (Monsoon) season.

An analysis of diurnal variation of sensible heat flux suggests that in each of the seasons, the heat flux follows a bell-shaped curve which attains a peak at a time between 1200-1300 IST. Sensible heat flux is found to be high in the Pre-monsoon season (214.30 ± 78.0 W/m^2) and minimum in monsoon season (105.47 ± 64.64 W/m^2), which is consistent with the study of Raman et al. (2003). However, the magnitude of both the average maximum and minimum values of heat flux are found to be significantly higher at Ranchi as compare to those obtained over another Indian region Lucknow (Ramana et al., 2003).

The observational behavior of σ_u, σ_v and σ_w normalized by friction velocity (u_*) with respect to stability parameter is analyzed in different seasons and wind speed regimes under stable and unstable conditions. In the near-neutral to moderate stable/unstable conditions, the values of σ_i/u_* ($i = u, v, w$) do not vary significantly and appear to be independent of stability. The corresponding maximum (minimum) average values are found to be 2.54(2.30), 2.45(2.01), 1.35(1.11). However, they are observed to increase with increasing stability/instability in moderate to strongly stable/unstable conditions. A good correlation between σ_i/u_* and ζ is observed in both the wind regimes in all the four seasons, which is in agreement with classical 1/3 power law. Empirical relationships for σ_i/u_* as functions of ζ under different wind and stability regimes in different seasons are proposed. The proposed empirical formulations have been evaluated using the turbulence measurements obtained from the seasons other than the one for which the formulations are developed. The analysis suggests that the bias introduced due to the use of one set of formulations in the other seasons is relatively small and one can eventually use the empirical formulations developed for a season into the other seasons without introducing significant error.

Acknowledgements

This work is partially supported by J C Bose Fellowship to M. S. from DST-SERB, Government of India (SB/S2/JCB - 79/2014). The raw turbulence data used in this study can be obtained from the Indian National Centre for Ocean Information Services (http://www.incois.gov.in/portal/datainfo/ctczdata.jsp) upon request.

References

Arya, S. P. S.: (1988), 'Introduction to Micrometeorology', *Academic Press*, pp.328.

Agarwal, P., Yadav, A. K., Gulati, A., Raman, S., Rao, S., Singh, M. P., Nigam, S., Reddy, N.: (1995), 'Surface layer turbulence processes in low wind speeds over land', Atmos. Environ. 29, 2089–2098.

Anfossi, D., Alessandrini, S., TriniCastelli, S., Ferrero, E., Oettl, D., Degrazia, G.: (2006), 'Tracer dispersion simulation in low wind speed conditions with a new 2D Langevin equation system', *Atmos. Environ.* **40**, 1112-1122.

Aditi and Sharan, M.: (2007), 'Analysis of Weak Wind Stable Conditions from the Observations of the Land Surface Processes Experiment at Anand in India', *Pure. Appl. Geophys*. **164**, 1811-1837.

Babić, K., Rotach, M. W., Klaić, Z. B.: (2016a), 'Evaluation of local similarity theory in the wintertime nocturnal boundary layer over heterogeneous surface', *Agric. Forest Meteorol.* **228-229**: 164-179.

Babić, N., Večenaj, Ž., De Wekker, S. F. J.: (2016b), 'Flux-variance similarity in complex terrain and its sensitivity to different methods of treating non-stationarity', *Boundary-Layer Meteorol*. **159**: 123-145.

Chang, J. C. and Hanna, S. R.: (2004), 'Air quality model performance', *Meteorol. Atmos. Phys.* **87**, 167-196.

Cheng, Y. G. and Brutsaert, W.: (2005), 'Flux-Profile Relationships for Wind Speed and Temperature in the Stable Atmospheric Boundary Layer', *Boundary-Layer Meteorol*. **114,** 519-538.

Dwivedi, A. K., Chandra, S., Kumar, M., Kumar, S. and Kumar, N. V. P. K.: (2014), 'Spectral Analysis of Wind and Temperature Components during Lightning in Pre-monsoon Season over Ranchi', *Meteor. Atmos. Phys.* **127**, 95–105.

Franceschi, M. de, Zardi, D., Tagliazucca, M., Tampieri, F.: (2009), ‘Analysis of second-order moments in surface layer turbulence in an Alpine valley’, *Q. J. R. Meteorol. Soc.* **135**, 1750–1765.

Giorgi, E., Coppola, E., Solmon, F., Mariotti, L., Sylla, M. B., Bi, X., Elguindi, N., Diro, G. T., Nair, V., Giuliani, G., Turuncoglu, U. U., Cozzini, S., Guttler, I., O’Brien, T. A., Tawfik, A. B., Shalaby, A., Zakey, A. S., Steiner, A. L., Stordal, F., Sloan, L. C. and Brankovic, C.: (2012), ‘RegCM4: Model Description and Preliminary Tests over Multiple CORDEX Domains’, *Cli. Res.* **52**, 7-29.

Gopalakrishnan, S. G., Sharan, M., McNider, R. T., and Singh, M. P.: (1998), ‘Study of radiative and turbulent processes in the stable boundary layer under weak wind conditions’, *J. Atmos. Sci.* **55,** 954–960.

Gopalakrishnan, S. G., Marks Jr. F. D., Zhang, J. A., Zhang, X., Bao, J. W. and Tallapragada, V.: (2013), ‘A study of the impacts of vertical diffusion on the structure and intensity of the tropical cyclones using the high-resolution HWRF system’, *J. Atmos. Sci.* **70**, 524–541.

Grachev, A. A., Andreas, E. L., Fairall, C. W., Guest, P. S. and Persson, P. O. G.: (2007), ‘SHEBA: Flux-Profile Relationships in Stable Atmospheric Boundary Layer’, *Boundary-Layer Meteorol*. **124**, 315-333.

Grachev, A. A., Andreas, E. L, Fairall, C. W., Guest, P. S., Persson, P. O. G.: (2013), ‘The critical Richardson number and limits of applicability of local similarity theory in the stable boundary layer’, *Boundary-Layer Meteorol*. **147**, 51-82.

Grachev, A. A., Leo, L. S., Fernando, H. J. S., Fairall, C.W., Creegan, E., Blomquist, B.W., Christman, A. J., Hocut, C. M. (2018), ‘Air-sea/land interaction in the coastal zone’, Boundary-Layer Meteorol. 167, 181-210.

Hanna, S. R., Briggs, G. A. and Hosker Jr., R. P.: (1982), ‘Handbook on Atmospheric Diffusion’, U.S. Dept. of Energy report COE/TIC-11223, Washington, DC.

Holmes, N. S. and Morawska, L.: (2006), ‘A Review of Dispersion Modelling and its Application to the Dispersion of Particles: An Overview of Different Dispersion Models Available’, *Atmos. Environ.* **40**, 5902-5928.

Kaimal, J. C., Finnigan, J. J.: (1994), ‘Atmospheric boundary layer flows: Their structure and measurements’, Oxford University Press, New York and Oxford, 289 pp.

Klipp, C. L. and Mahrt, L.: (2004), ‘Flux-Gradient Relationship, Self-Correlation and Intermittency in the Stable Boundary Layer’, *Q. J. R. Meteorol. Soc.* **130**, 2087–2103.

Krishnan, P. and Kunhikrishnan, P. K.: (2002), ‘Some Characteristics of Atmospheric Surface Layer over a Tropical Inland Region during Southwest Monsoon Period’, *Atmos. Res.* **62**, 11–124.

Kunhikrshnan, P. K.: (1990), ‘Studies of atmospheric boundary layer’, Ph.D. Thesis, University of Kerala, India, pp 187.

Kumar, P. and Sharan, M.: (2010), ‘An Analytical Model for Dispersion of Pollutants from a Continuous Source in the Atmospheric Boundary Layer’, *Proc. R. Soc. A* **466**, 383-406.

Kumar, P. and Sharan, M.: (2012), ‘An Analysis for the Applicability of Monin–Obukhov Similarity Theory in Stable Conditions. *J. Atmos. Sci.* **69**, 1910–1915.

Kumar, A. and Goyal, P.: (2014), ‘Air Quality Prediction of PM10 through Analytical Dispersion Model for Delhi’, *Aero. Air Qua. Res.* **14**, 1484-1499.

Kumar, P., Feiz, A. A., Singh, S. K., Ngae, P. and Turbelin, G.: (2015), ‘Reconstruction of an atmospheric tracer source in an urban-like environment’, *J. Geophys. Res. Atmos.* **120**, 12589–12604.

Luhar, A. K., Hurley, P. J. and Rayner, K. N.: (2009), ‘Modelling Near-Surface Low Winds over Land under Stable Conditions: Sensitivity Tests, Flux-Gradient Relationships, and Stability Parameters’, *Boundary-Layer Meteorol*. **130 (2)**, 249-274.

Luhar, A. K.: (2010), ‘Estimating Variances of Horizontal Wind Fluctuations in Stable Conditions’, *Boundary-Layer Meteorol*. **135**: 301–311.

Luhar, A. K.: (2011), ‘Analytical puff modelling of light-wind dispersion in stable and unstable conditions’, *Atmos. Environ.* **45**, 357–368.

Mahrt, L.: (1998), ‘Stratified Atmospheric Boundary Layers and Breakdown of Models’, *Theor. Comput. Fluid Dyn.* **11**, 263-279.

Mahrt, L.: (2008), ‘Bulk Formulation of Surface Fluxes Extended to Weak-Wind Stable Conditions’, *Q. J. R. Meteorol. Soc.* **134**, 1-10.

Mahrt, L.: (2014), ‘Stably Stratified Atmospheric Boundary Layer’, *Annual Review of Fluid Mechanics* **46**, 23-45.

Martins, C. A., Moraes, O. L. L., Acevedo, O. C. and Degrazia, G. A.: (2009), 'Turbulence Intensity Parameters over a very Complex Terrain', *Boundary-Layer Meteorol*. **133**, 35–45.

Moraes, O. L. L., Acevedo, O. C., Degrazia, G. A., Anfossi, D., Da Silva, R., Anabor, V.: (2005), 'Surface layer turbulence parameters over a complex terrain', *Atmos. Environ.* **39**, 3103–3112.

Monin, A. S. and Obukhov, A. M.: (1954), 'Osnovnye Zakonomernosti Turbulentnogo Peremeshivanija v Prizemnom sloe Atmosfery (Basic Laws of Turbulent Mixing in the Atmosphere near the Ground)', *Trudy geofiz. Inst. AN SSSR* **24 (151),** 163-187.

Nadeau, D. F., Pardyjak, E. R., Higgins, C. W., Parlange, M. B.: (2013), 'Similarity scaling over a steep alpine slope', *Boundary-Layer Meteorol*. **147**: 401-419.

Panofsky, H. A., Tennekes, H., Lenschow, D. H. and Wyngaard, J. C.: (1977), 'The Characteristics of Turbulent Velocity Components in the Surface Layer under Convective Conditions', *Boundary-Layer Meteorol*. **11**, 355–361.

Panofsky H., Dutton, J. A.: (1984), 'Atmospheric turbulence: models and methods for engineers and scientists', Wiley, New York, p 397

Pahlow, M., Parlange, M. B. and Porté-Agel, F.: (2001), 'On Monin-Obukhov Similarity in the Stable Atmospheric Boundary Layer', *Boundary-Layer Meteorol*. **99**, 225-248.

Pandey, G., Sharan, M.: (2017), 'Performance evaluation of dispersion parameterization schemes in the plume simulation of FFT-07 diffusion experiment', *Atmos. Environ.* **172**, 32–46.

Prasad, K.B.R.R.H., Srinivas, C.V., Singh, A.B., Naidu, C.V., Baskaran, R., and Venkatraman, B.: (2018), 'Turbulence characteristics of surface boundary layer over the Kalpakkam tropical coastal station, India', *Meteorol. Atmos. Phys.*, https://doi.org/10.1007/s00703-018-0605-6.

Ramachandran, R., Prakash, J. W. J., Sen Gupta, K., Nair, K. N., and Kunhikrishnan, P. K.: (1994), 'Variability of Surface Roughness and Turbulence Intensities at a Coastal Site in India', *Boundary-Layer Meteorol.* **70**, 385–400.

Qian,W., Venkatram, A.: (2011), 'Performance of steady-state dispersion models under low wind-speed conditions', *Boundary-Layer Meteorol.* **138**, 478-491.

Ramana, M.V., Krishnan, P., Kunhikrishnan, P. K. (2004), 'Surface boundary layer characteristics over a tropical inland station: seasonal features', *Boundary-Layer Meteorol.***111**:153–175.

Rannik Ü.: (1998), 'On the surface layer similarity at a complex forest site', *J. Geophys. Res*. **103(D8)**, 8685-8697.

Rao, K. G. and Narasimha, R.: (2006), 'Heat-flux Scaling for Weakly Forced Turbulent Convection in Atmosphere', *J. Fluid Mech.* **547**, 115–135.

Skamarock, W. C., Klemp, J. B., Dudhia, J., Gill, D. O., Barker, D. M., Duda, M. G., Huang, X., Wang, W. and Powers, J. G.: (2008), 'A Description of the Advanced Research WRF Version 3', Tech. Rep. TN-475+STR, NCAR, 133 pp.

Sharan, M., Singh, M.P., Yadav, A.K., Agarwal, P., Nigam, S.: (1996), 'A mathematical model for dispersion of air pollutants in low wind conditions', *Atmos. Environ.* **30**, 1209-1220.

Sharan, M., Gopalakrishnan, S. G. and McNider, R. T.: (1997), 'A Local Parameterization Scheme for σ_w under Stable Conditions', *J. Appl. Meteorol*. **36**, 545-559.

Sharan, M., Singh, S.K., Issartel, J.P.: (2012), 'Least square data assimilation for identification of the point-source emissions', *Pure Appl. Geophys.* **169**, 483-497.

Srivastava, P. and Sharan, M.: (2015), 'Characteristics of Drag Coefficient over a Tropical Environment in Convective Conditions', *J. Atmos. Sci*. **72**, 4903-4913.

Stiperski, I., Rotach, M.W.: (2016), 'On the measurement of turbulence over complex mountainous terrain', *Boundary-Layer Meteorol* **159**: 97-121.

Srivastava, P., and Sharan, M. (2019), 'Analysis of dual nature of heat flux predicted by Monin-Obukhov similarity theory: An impact of empirical forms of stability correction functions. *J. Geophys. Res.: Atmos.*, **124**. https://doi.org/10.1029/2018JD029740

Trini Castelli, S., Falabino, S., Mortarini, L., Ferrero, E., Richiardone, R. and Anfossi, D.: (2014), 'Experimental Investigation of Surface-layer Parameters in Low Wind-speed Conditions in a Suburban Area', *Q. J. R. Meteorol. Soc.* **140**, 2023–2036.

Trini Castelli, S. and Falabino, S.: (2013), 'Parameterization of the Wind Velocity Fluctuation Standard Deviations in the Surface Layer in Low-wind Conditions', *Meteorol. Atmos. Phys.* **119**, 91–107.

Tyagi, B. and Satyanarayana, A.N.V.: (2013), 'Assessment of turbulent kinetic energy and boundary layer characteristics at a tropical Indian station Ranchi', *Asia Pac. J. Atmos. Sci.* **49**, 587–601.

Wood, C. R., Lacser, A., Barlow, J. F., Padhra, A., Belcher, S. E., Nemitz, E., Helfter, C., Famulari, D., Grimmond, C. S. B.: (2010), 'Turbulent flow at 190 m height above London during 2006-2008: A climatology and the applicability of similarity theory', *Boundary-Layer Meteorol* **137**: 77-9.

Yusup, Y.B., Daud, W. R. W., Zaharim, A., Talib, M. Z. M.: (2008), 'Structure of the atmospheric surface layer over an industrialized equatorial area', *Atmos. Res.* **90**, 70–77.

Zhang, J. A., Nolan, D. S., Rogers, R. F. and Tallapragada, V.: (2015), 'Evaluating the impact of improvements in the boundary layer parameterizations on hurricane intensity and structure forecasts in HWRF', *Mon. Wea. Rev.* **143**, 3136–315.

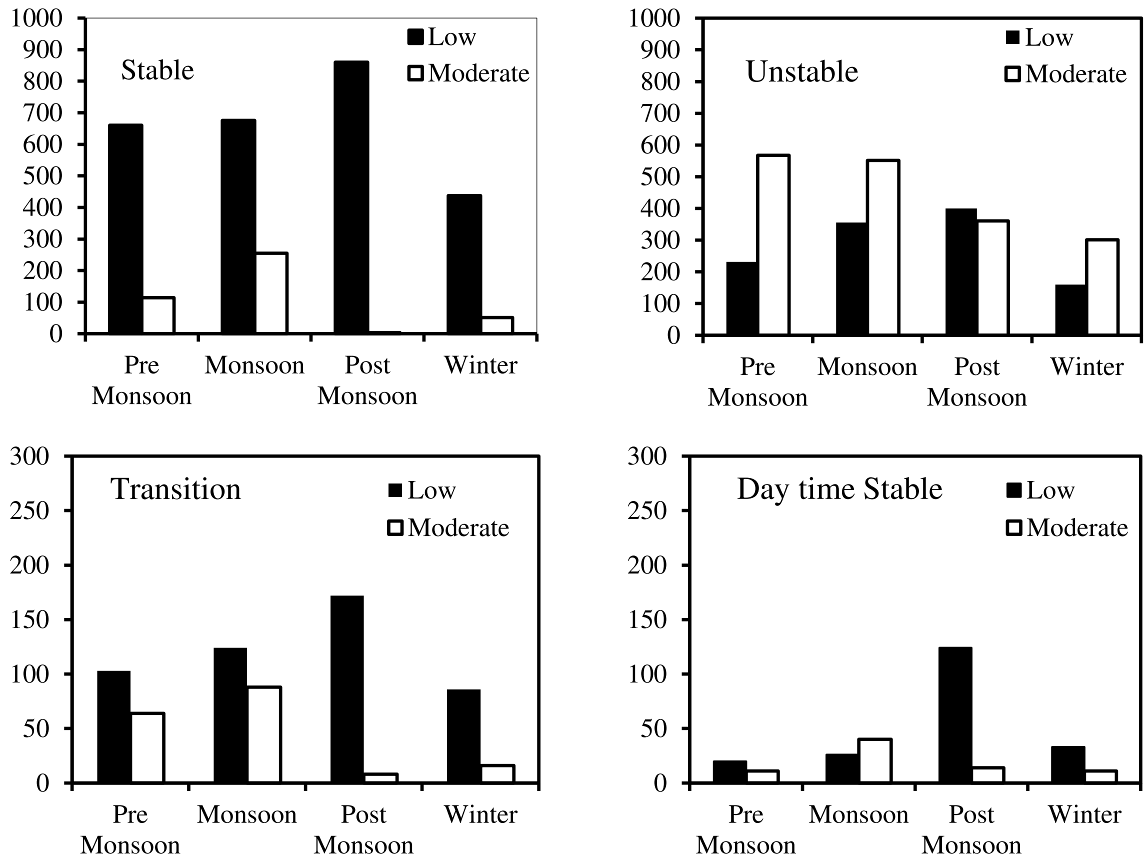

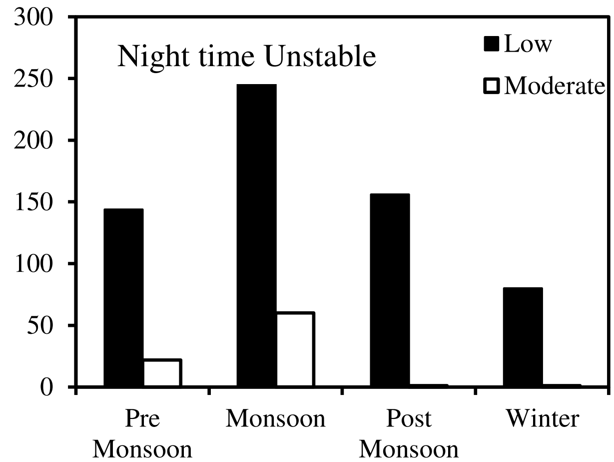

Figure 1: Histograms for quantitative description of the data in different stability and wind speed regimes in four seasons.

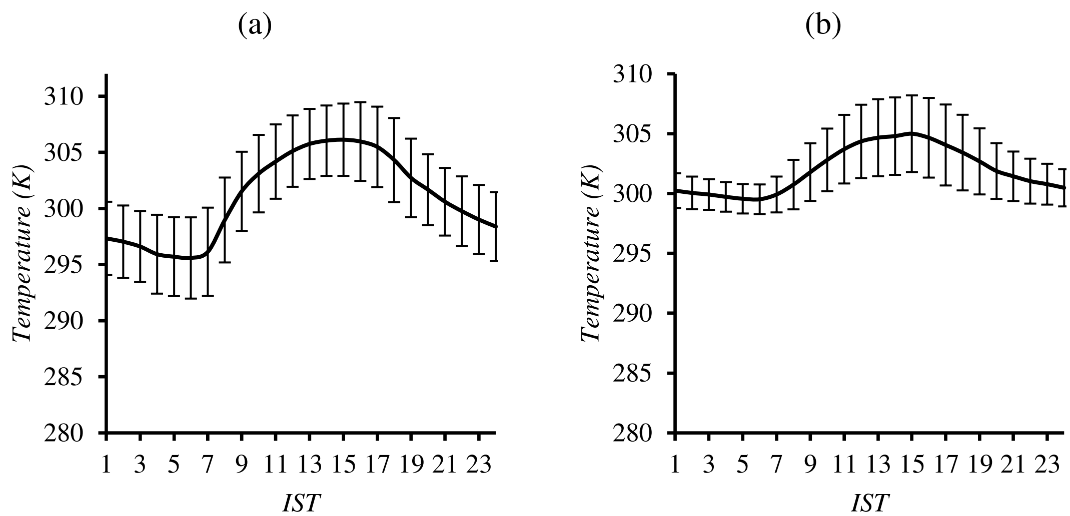

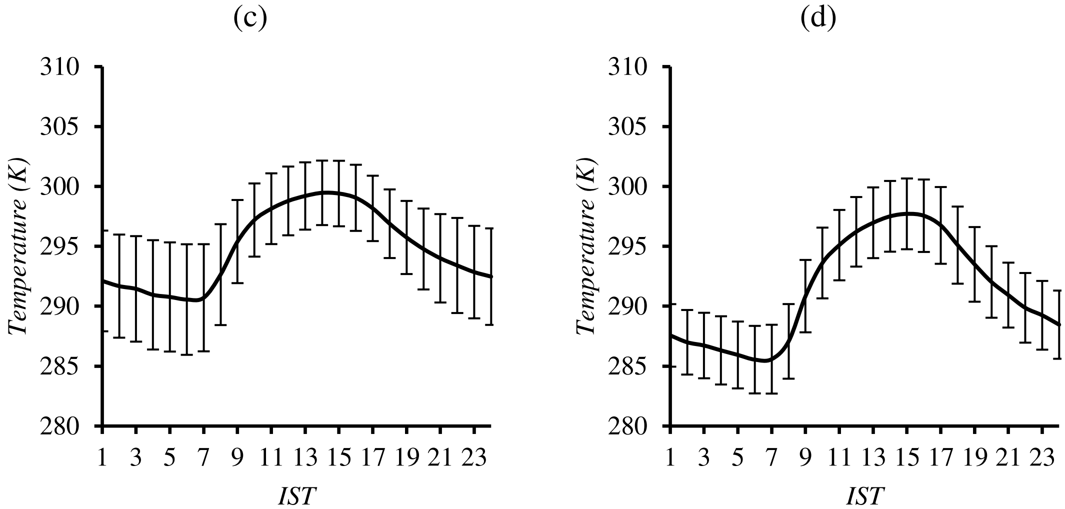

Figure 2: Diurnal variation of temperature (in Kelvin) in (a) Pre-monsoon, (b) Monsoon, (c) Post Monsoon, and (d) Winter season. In each of the panels, the vertical lines represent the error bars.

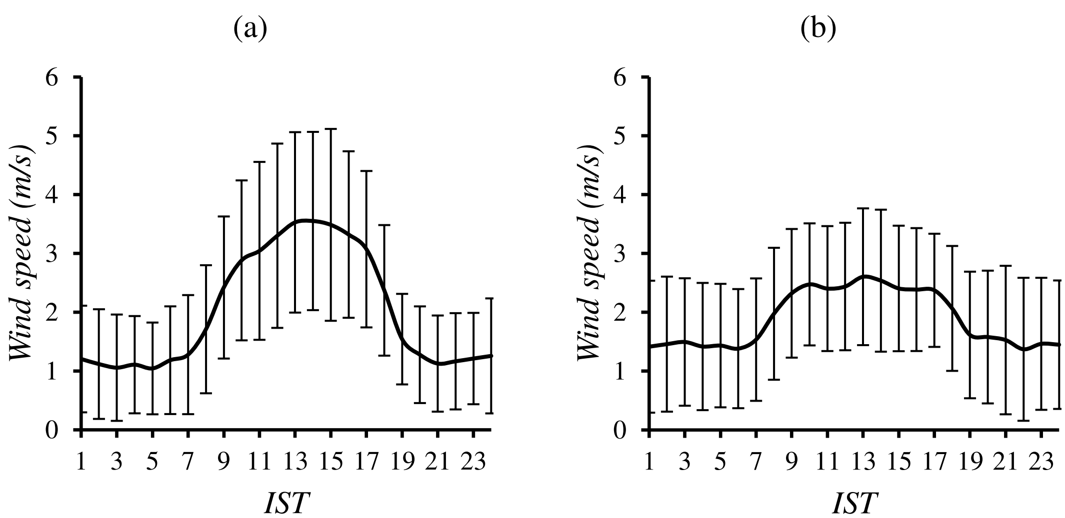

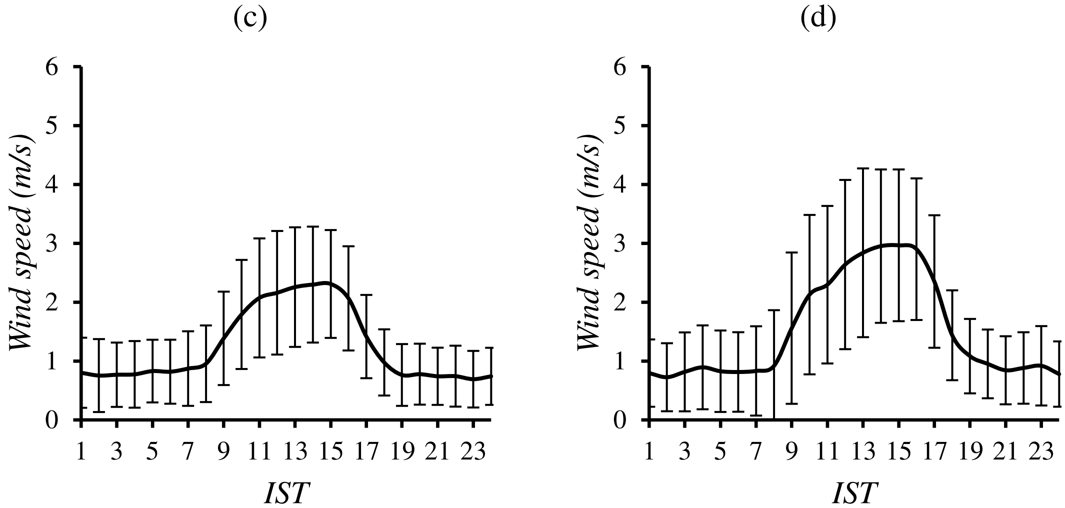

Figure 3: Diurnal variation of wind speed (in m/s) in (a) Pre-monsoon, (b) Monsoon, (c) Post-monsoon, and (d) Winter season. In each of the panels, the vertical lines represent the error bars.

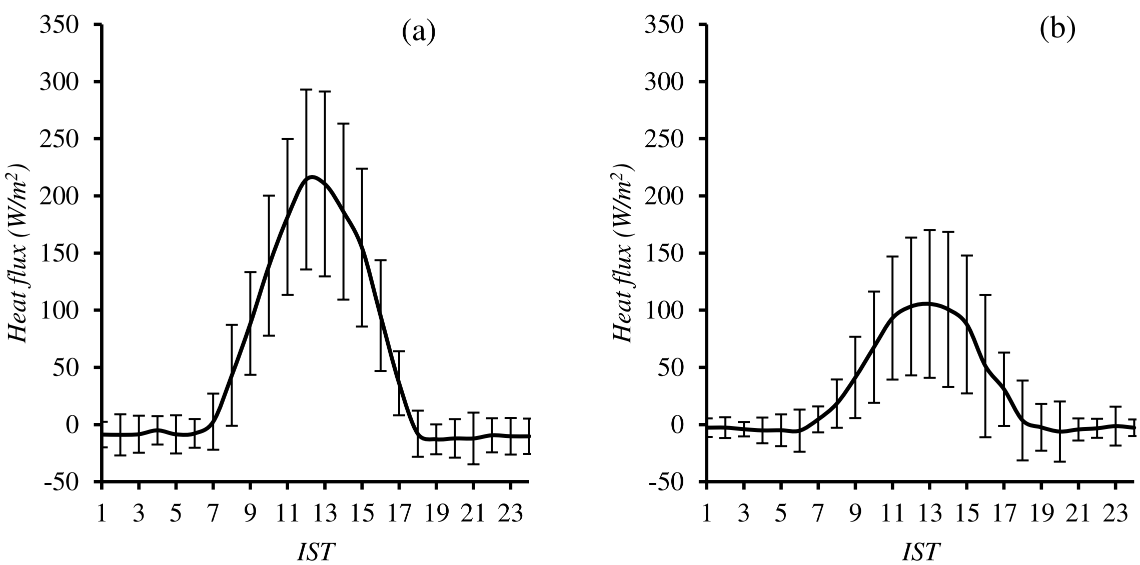

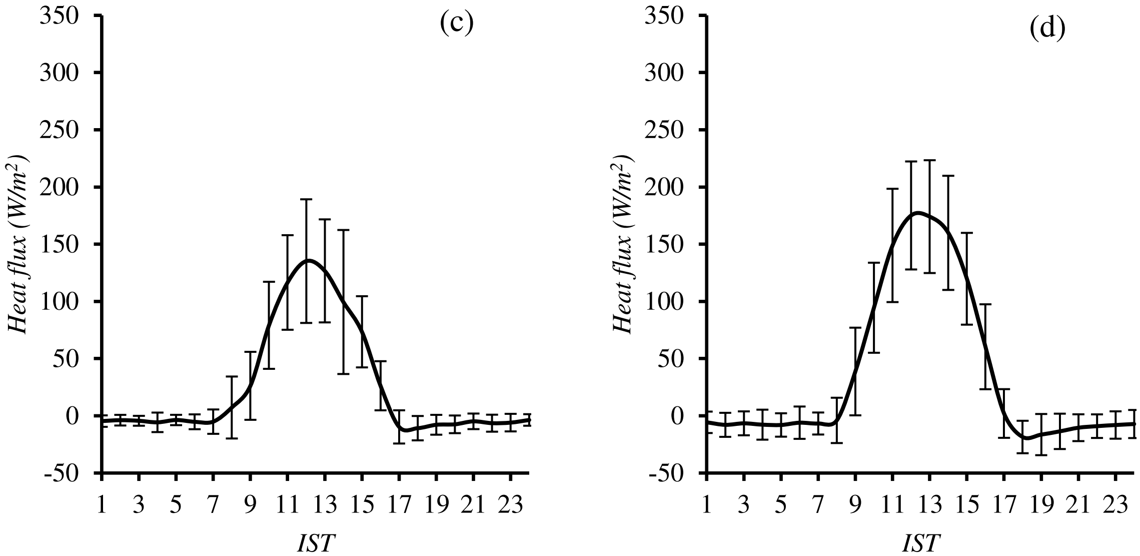

Figure 4: Diurnal variation of Heat flux (in W/m^2) in (a) Pre-monsoon, (b) Monsoon, (c) Post-monsoon, and (d) Winter season. In each of the panels, the vertical lines represent the error bars.

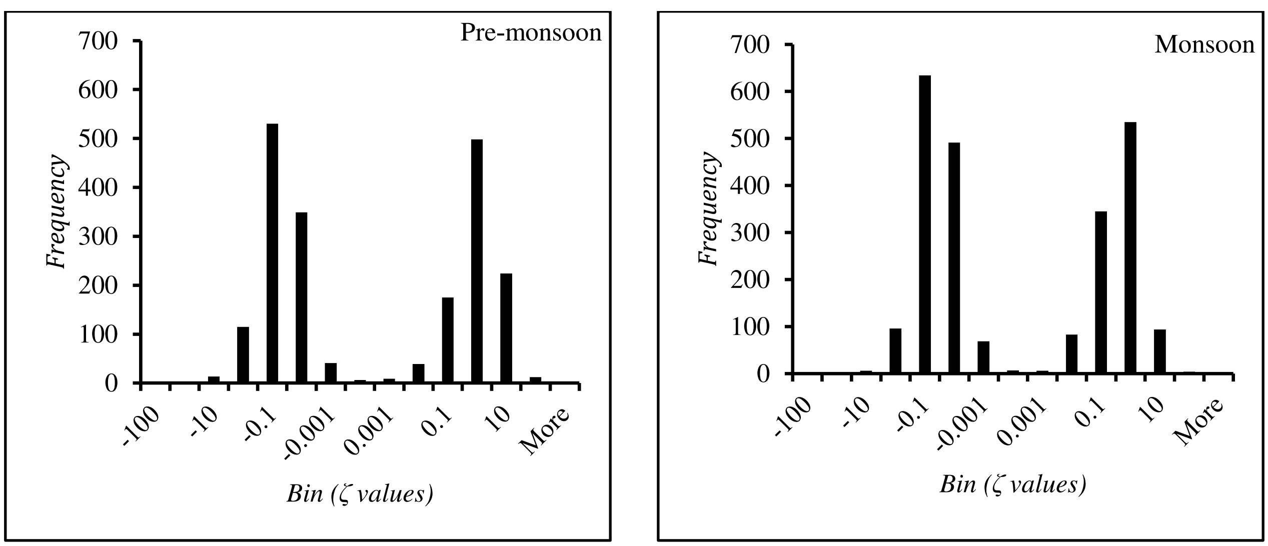

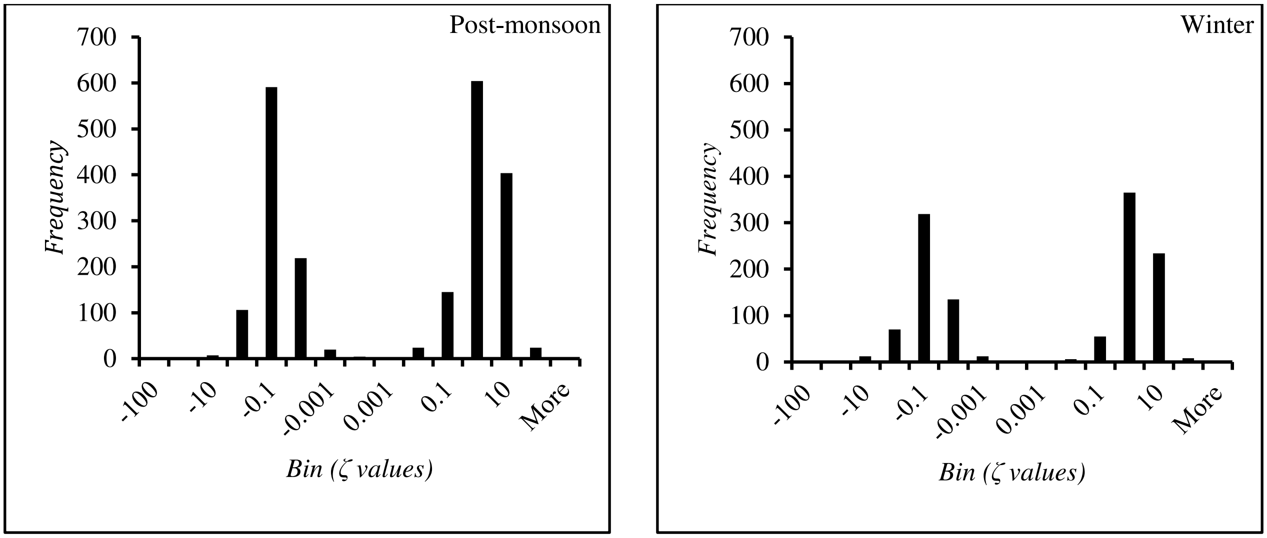

Figure 5: Frequency distribution of values of stability parameter in four seasons.

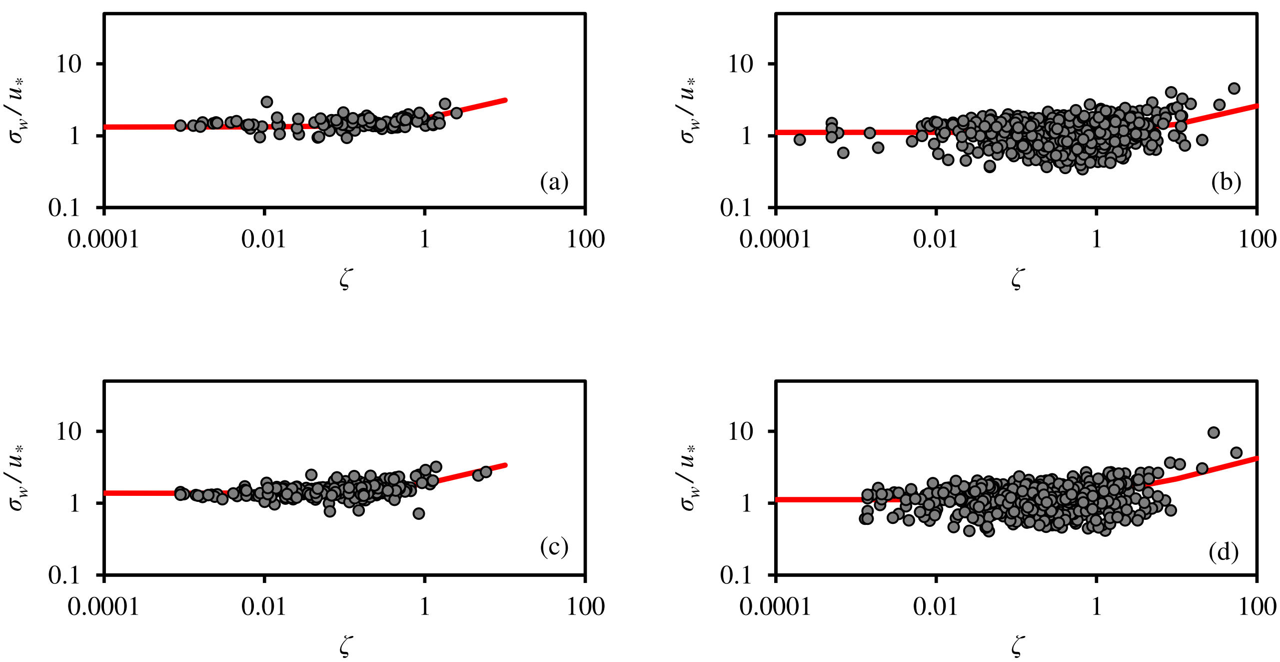

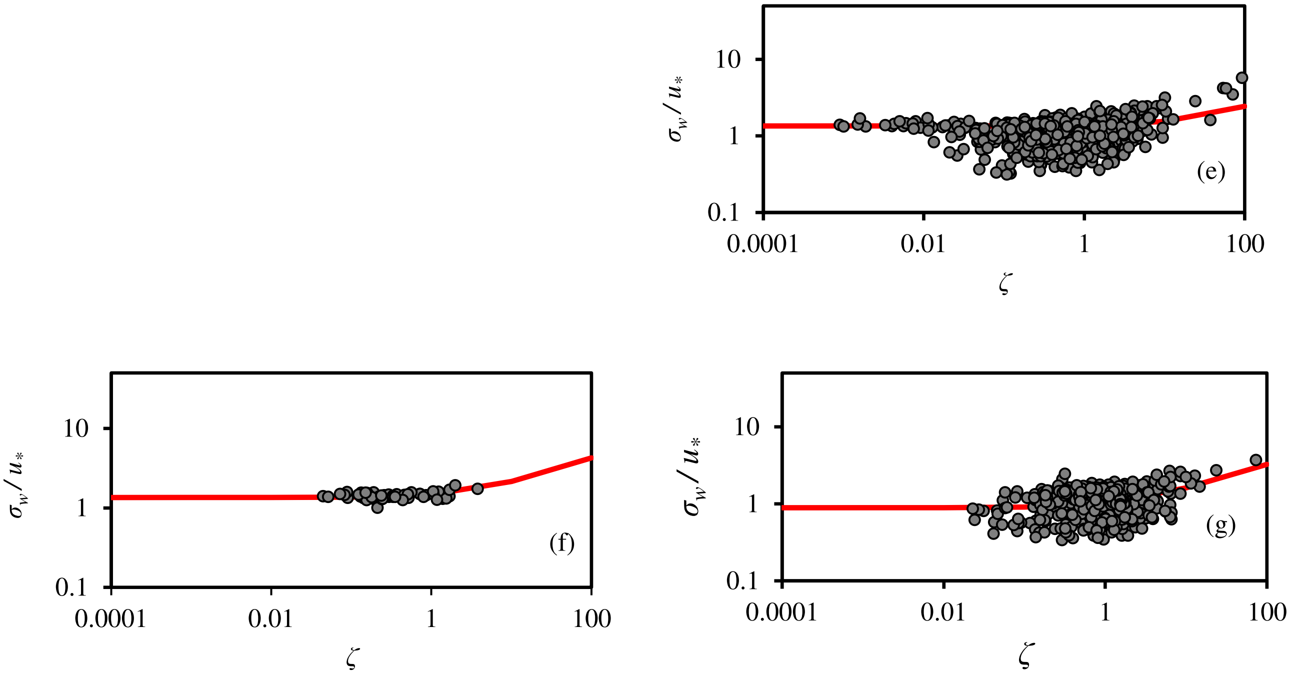

Fig. 6 Variation of the normalized standard deviations of the vertical velocity component σ_w/u_* versus the local Monin-Obukhov stability parameter ζ in the logarithmic axis for turbulence data over Ranchi from pre-monsoon (a, b), monsoon (c, d), post-monsoon (e) and winter (f, g) seasons under stable conditions (i.e. $\zeta > 0$). The left panels (a, c, f) correspond to moderate wind conditions; the right panels (b, d, e, g) represent low wind conditions. The continuous lines correspond to best-fit curves.

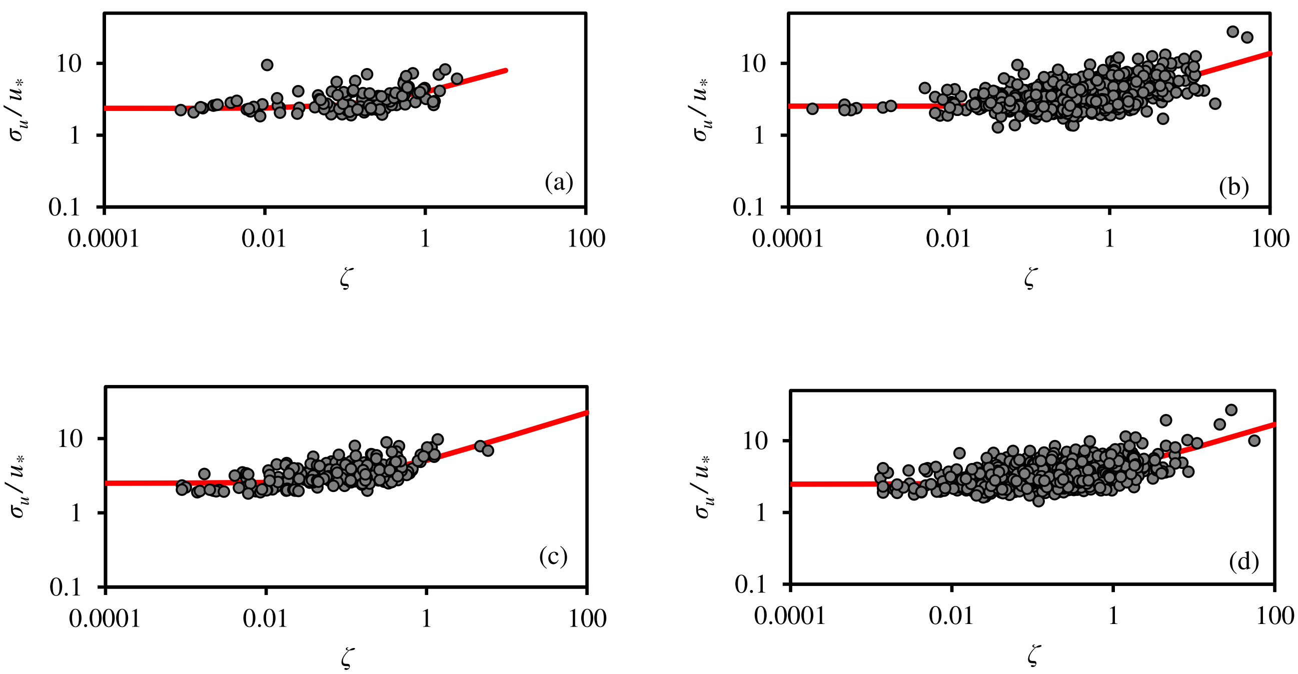

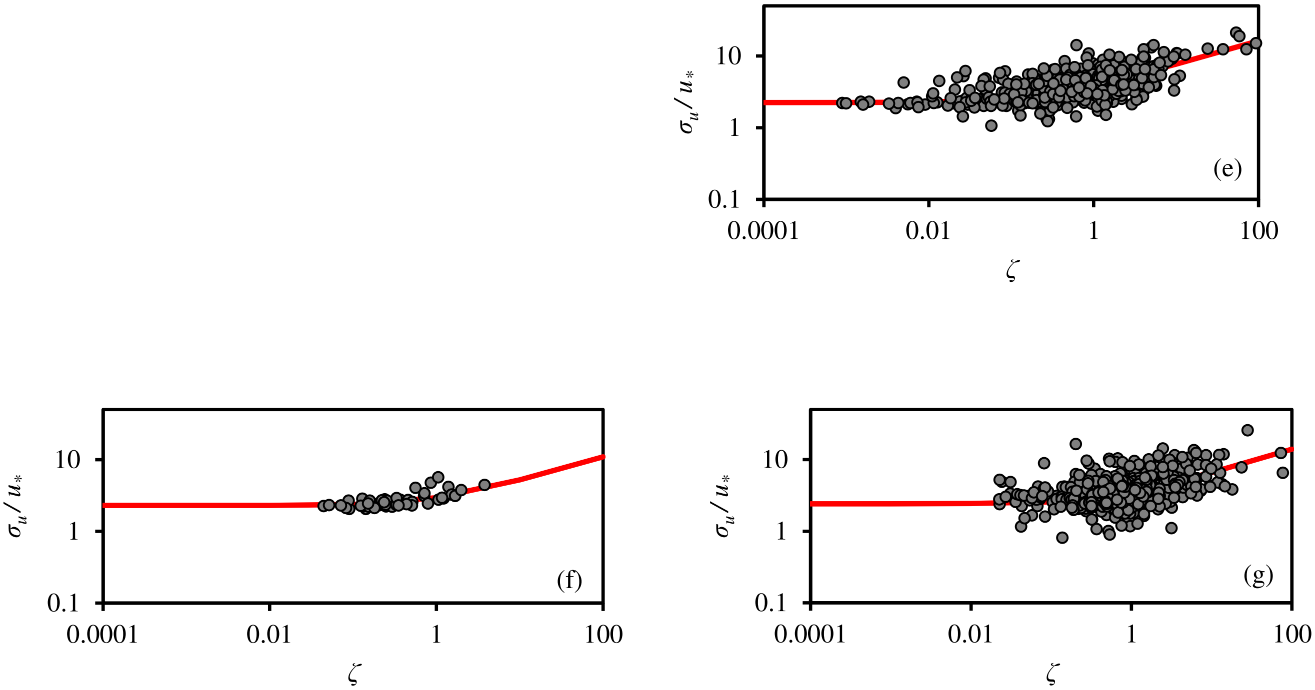

Fig. 7 Similar to Fig. 6, variation of σ_u/u_* with ζ for pre-monsoon (a, b), monsoon (c, d), post-monsoon (e) and winter (f, g) seasons under stable conditions. The left panels (a, c, f) correspond to moderate wind conditions; the right panels (b, d, e, g) represent low wind conditions. The continuous lines correspond to best-fit curves.

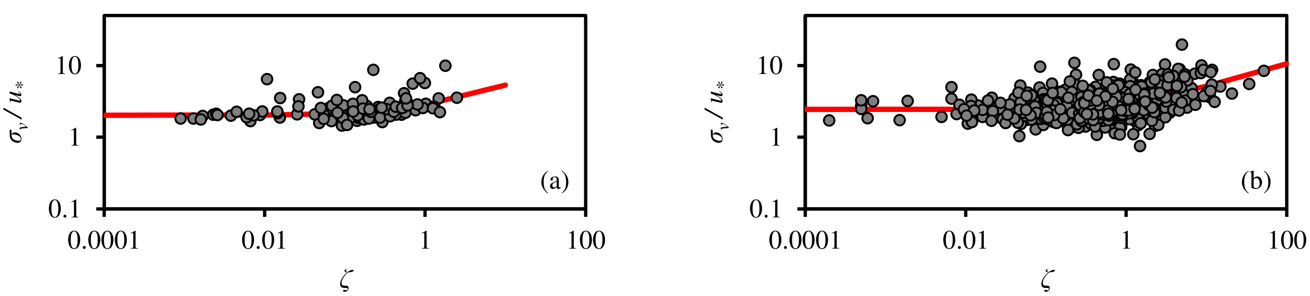

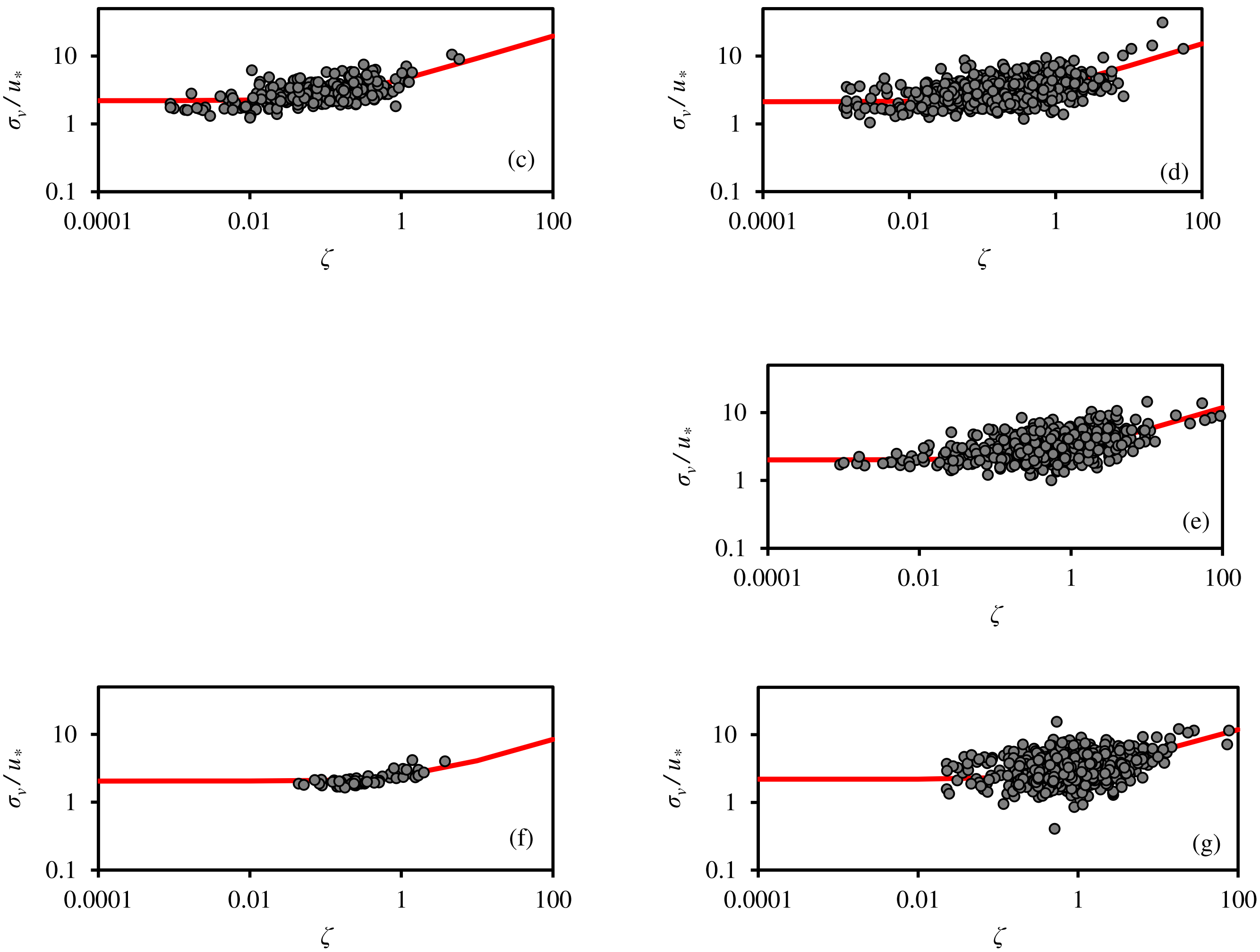

Fig. 8 Similar to Fig. 6, variation of σ_v / u_* with ζ for pre-monsoon (a, b), monsoon (c, d), post-monsoon (e) and winter (f, g) seasons under stable conditions. The left panels (a, c, f) correspond to moderate wind conditions; the right panels (b, d, e, g) represent low wind conditions.

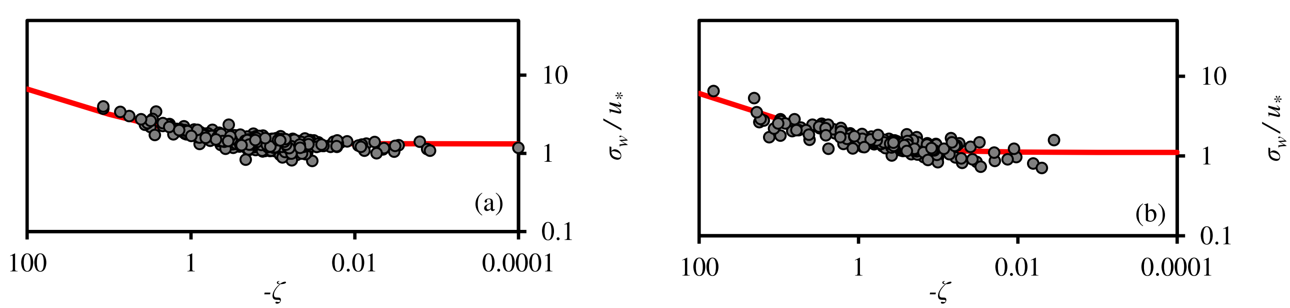

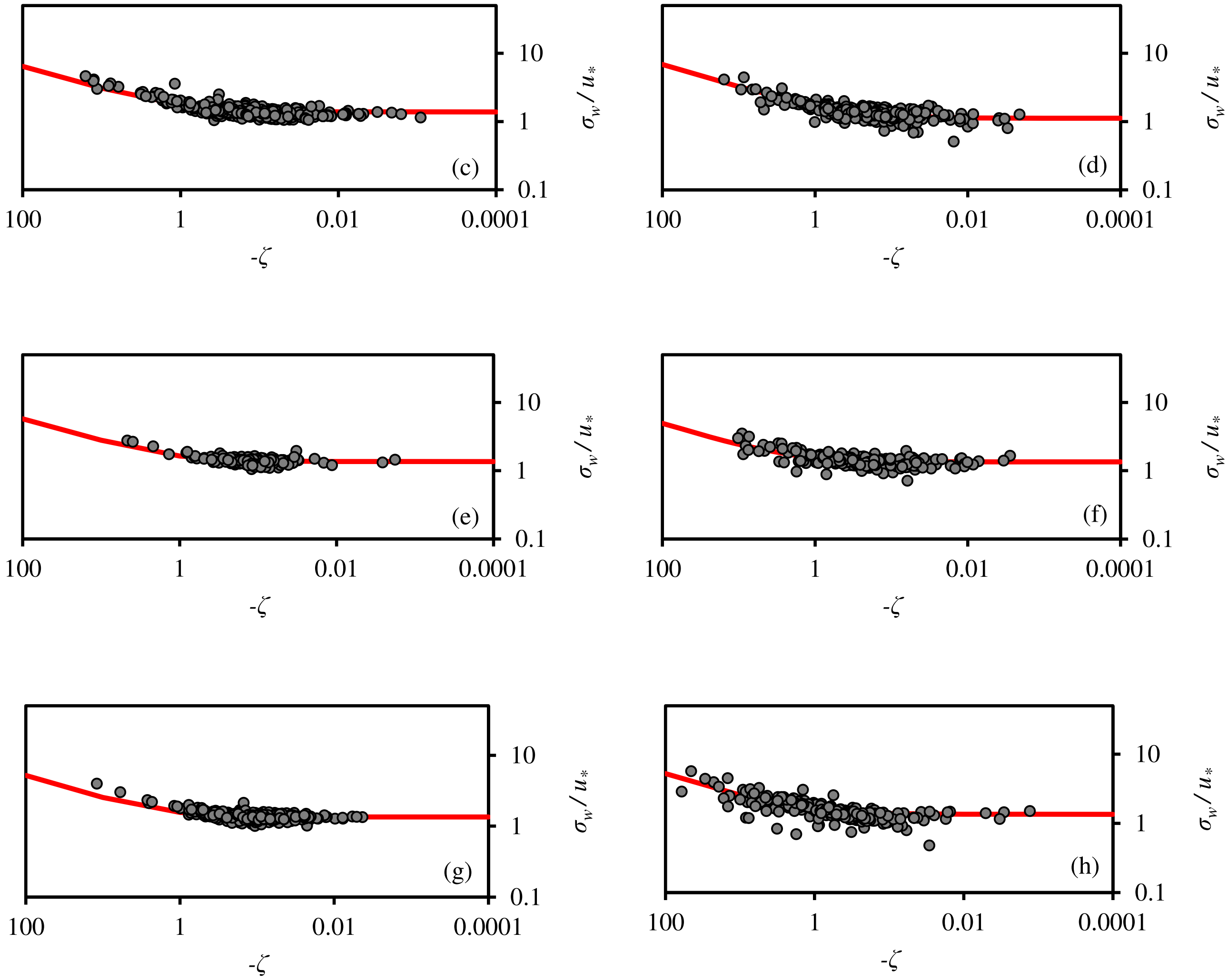

Fig. 9 Variation of the normalized standard deviations of the vertical velocity component σ_w/u_* versus the local Monin-Obukhov stability parameter ζ in the logarithmic axis for turbulence data over Ranchi from pre-monsoon (a, b), monsoon (c, d), post-monsoon (e, f) and winter (g, h) seasons under unstable conditions (i.e. $\zeta < 0$). The left panels (a, c, e, g) correspond to moderate wind conditions; the right panels (b, d, f, h) represent low wind conditions. The continuous lines correspond to best-fit curves.

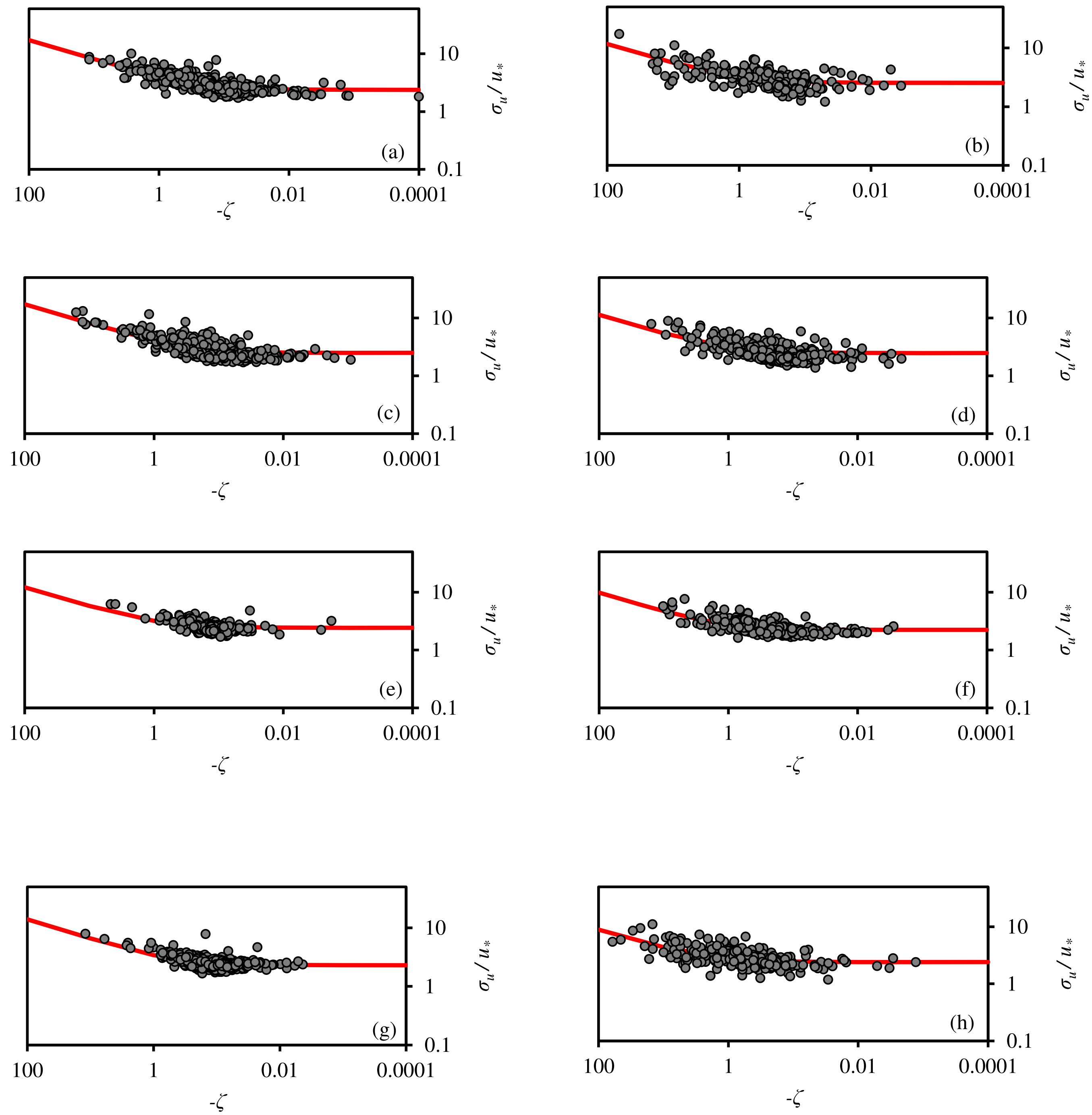

Fig. 10 Similar to Fig. 9**,** variation of σ_u/u_* versus ζ for pre-monsoon (a, b), monsoon (c, d), post-monsoon (e, f) and winter (g, h) seasons under unstable conditions. The left panels (a, c, e, g) correspond to moderate wind conditions; the right panels (b, d, f, h) represent low wind conditions.

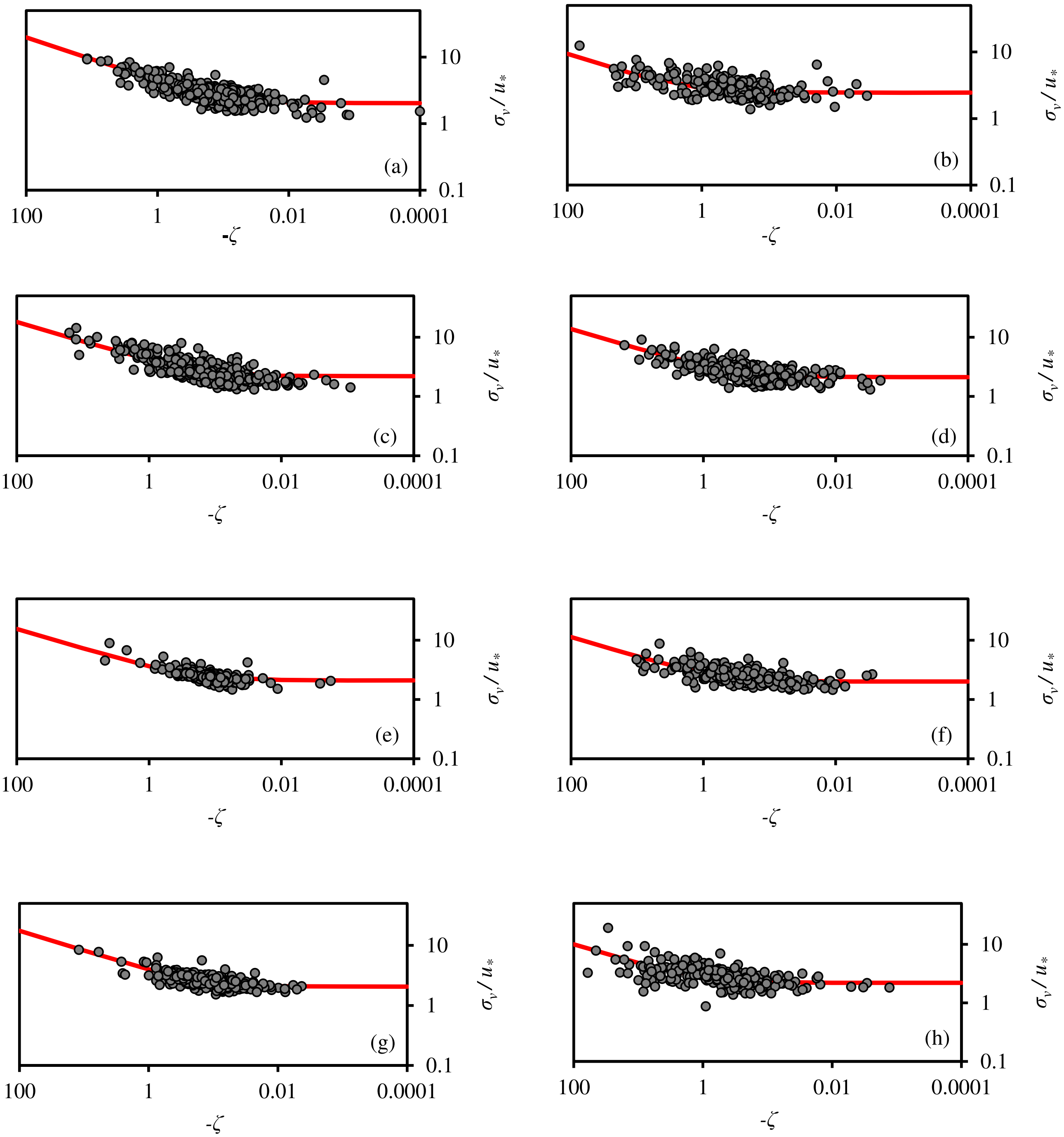

Fig. 11: Similar to Fig. 9, variation of σ_v / u_* versus ζ for pre-monsoon (a, b), monsoon (c, d), post-monsoon (e, f) and winter (g, h) seasons under unstable conditions. The left panels (a, c, e, g) correspond to moderate wind conditions; the right panels (b, d, f, h) represent low wind conditions.

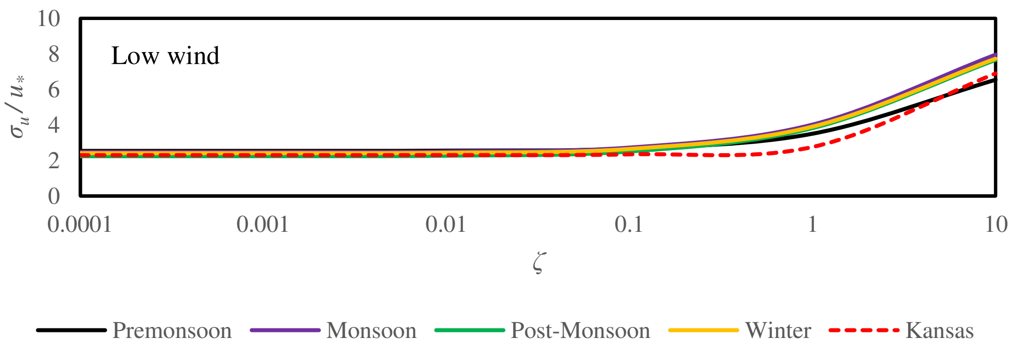
Low wind
σ_u / u_*
10
8
6
4
2
0
0.0001
0.001
0.01
0.1
1
10
ζ
Premonsoon
Monsoon
Post-Monsoon
Winter
Kansas

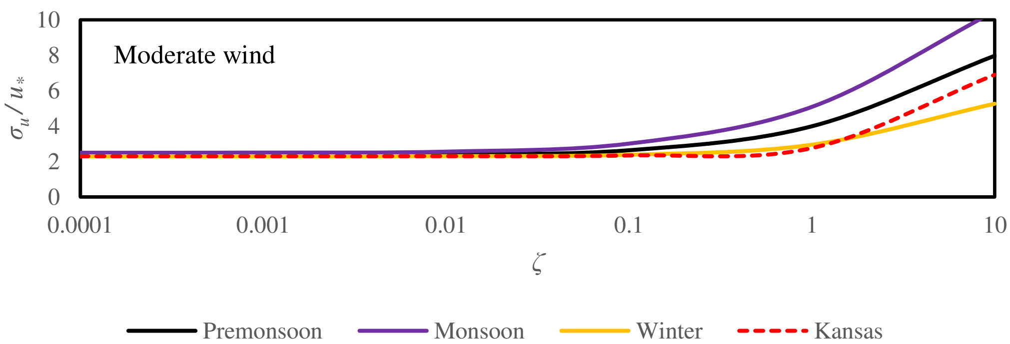
Moderate wind
σ_u / u_*
10
8
6
4
2
0
0.0001
0.001
0.01
0.1
1
10
ζ
Premonsoon
Monsoon
Winter
Kansas

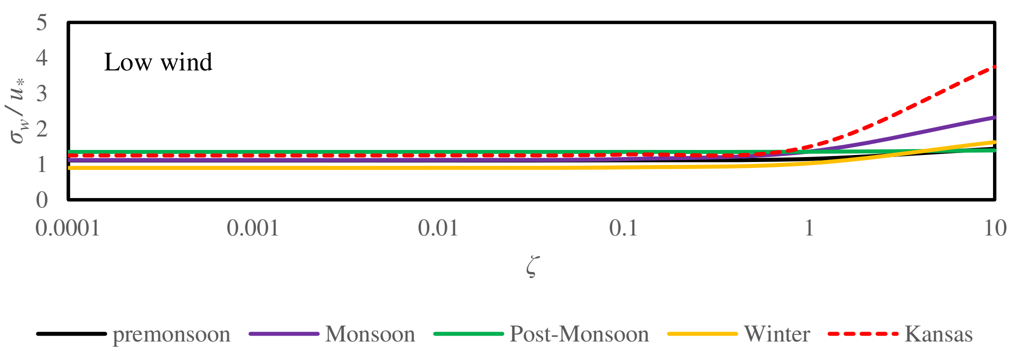
Low wind
σ_w / u_*
5
4
3
2
1
0
0.0001
0.001
0.01
0.1
1
10
ζ
premonsoon
Monsoon
Post-Monsoon
Winter
Kansas

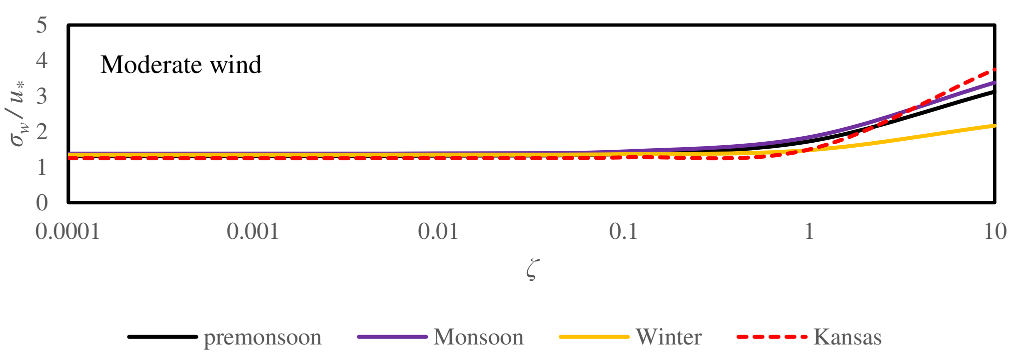
Moderate wind
σ_w / u_*
5
4
3
2
1
0
0.0001
0.001
0.01
0.1
1
10
ζ
premonsoon
Monsoon
Winter
Kansas

Fig. 12: Comparison of functional relationships of $\sigma_{u,w}/u_*$ with respect to ζ derived from present data set in different seasons (solid lines with different colours) with those suggested by Kaimal and Finnigan (1994) (red dashed lines) under stable conditions.

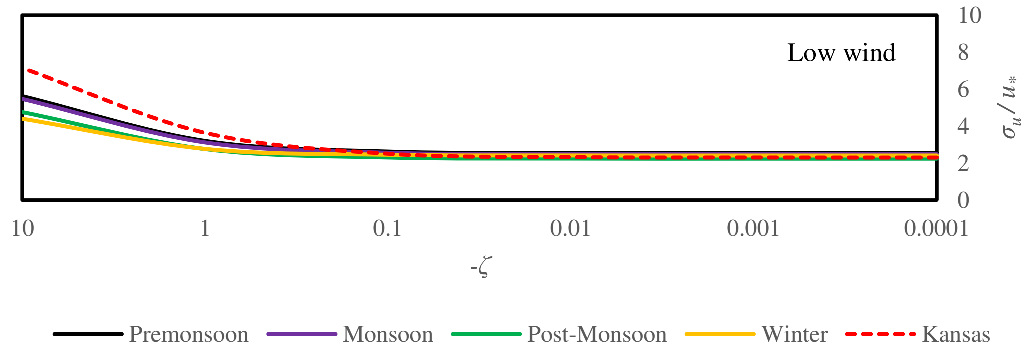
Low wind
10
8
6
4
2
0
σ_u / u_*
10
1
0.1
0.01
0.001
0.0001
-ζ
Premonsoon
Monsoon
Post-Monsoon
Winter
Kansas

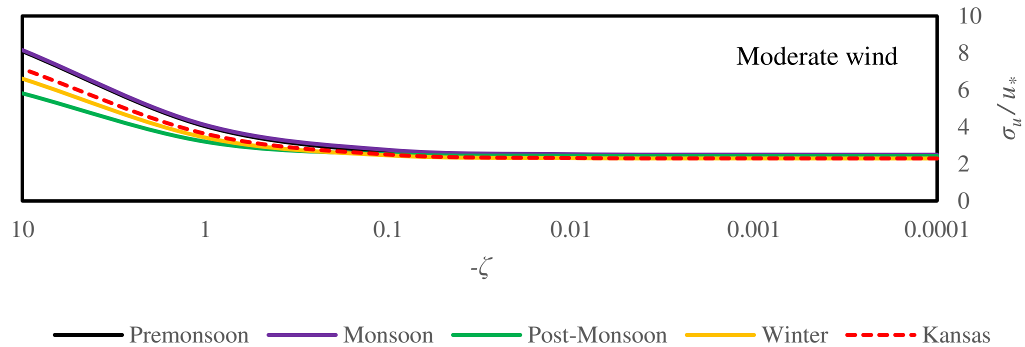
Moderate wind
10
8
6
4
2
0
σ_u / u_*
10
1
0.1
0.01
0.001
0.0001
-ζ
Premonsoon
Monsoon
Post-Monsoon
Winter
Kansas

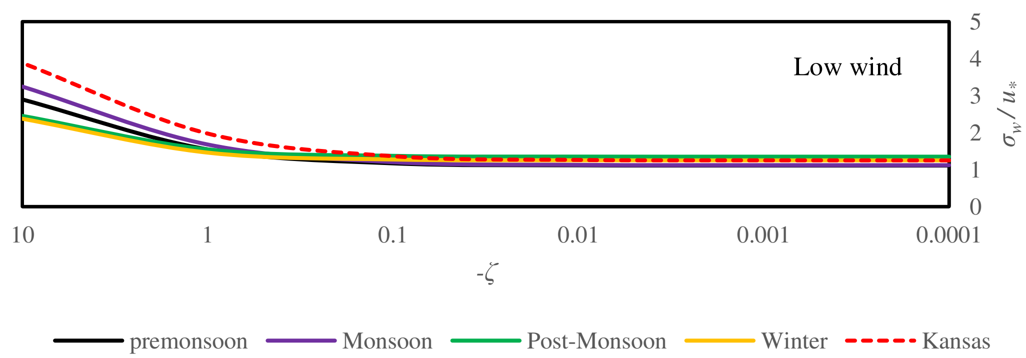
Low wind
5
4
3
2
1
0
σ_w / u_*
10
1
0.1
0.01
0.001
0.0001
-ζ
premonsoon
Monsoon
Post-Monsoon
Winter
Kansas

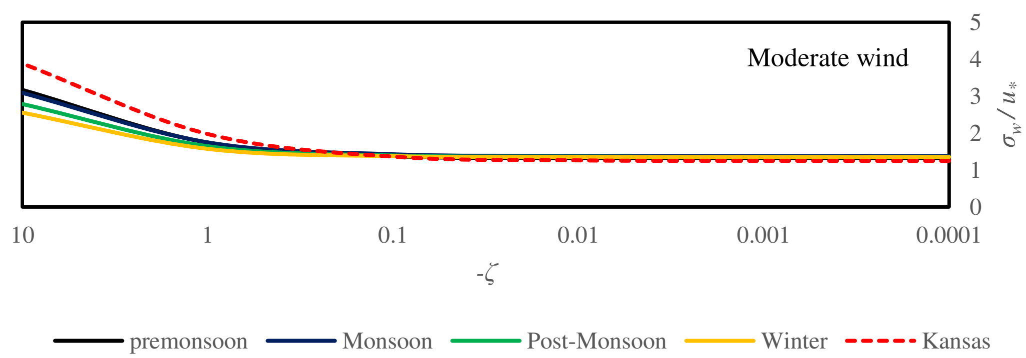
Moderate wind
5
4
3
2
1
0
σ_w / u_*
10
1
0.1
0.01
0.001
0.0001
-ζ
premonsoon
Monsoon
Post-Monsoon
Winter
Kansas

Fig. 13 Similar to Fig. 12, comparison of functional relationships of $\sigma_{u,w}/u_*$ with respect to ζ derived from present data set in different seasons with those suggested by Kaimal and Finnigan (1994) under unstable conditions.

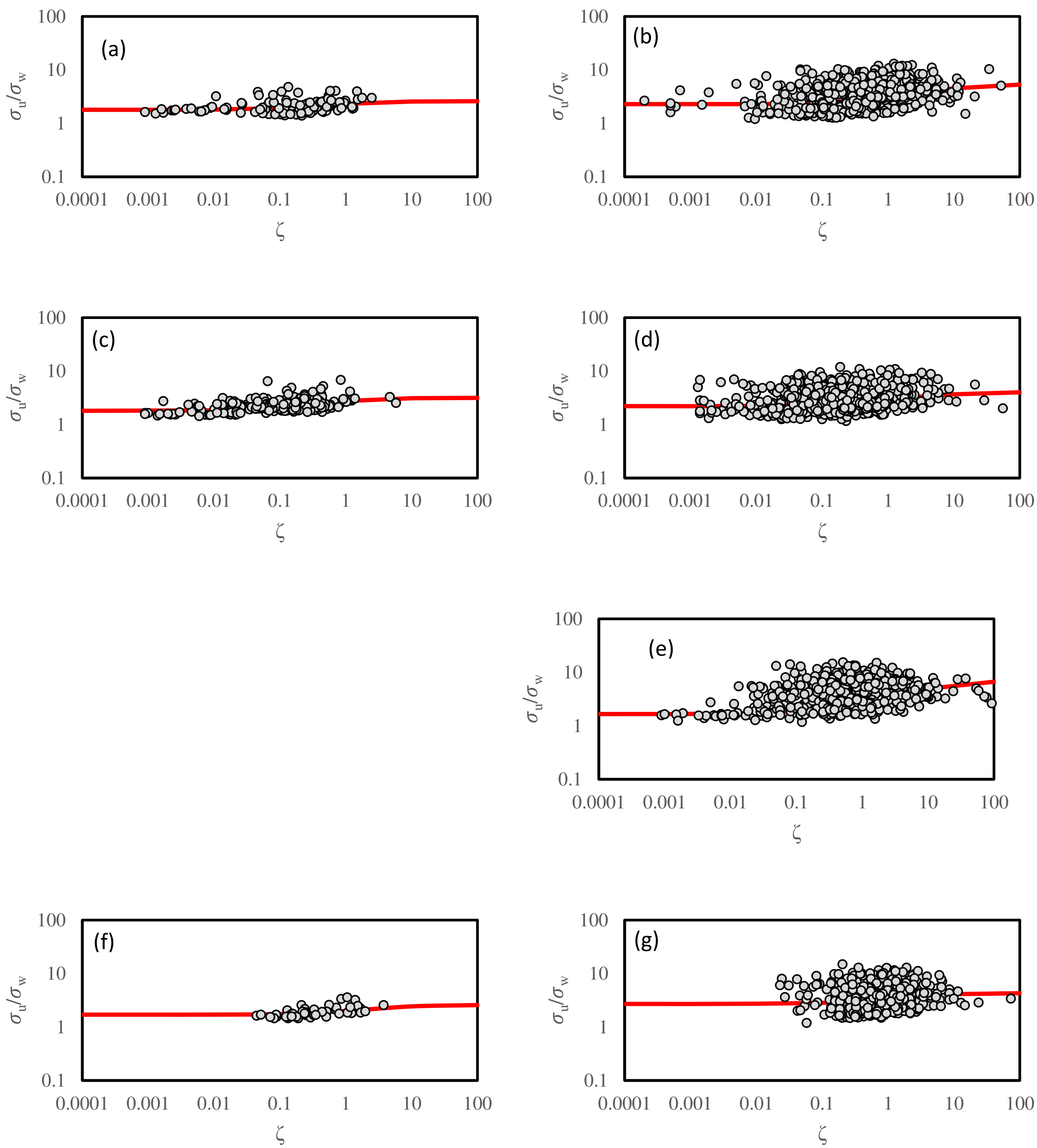

Fig. 14 Variation of $\varphi_u/\varphi_w = \sigma_u/\sigma_w$ with ζ (which is not affected by the self-correlation) for pre-monsoon (a, b), monsoon (c, d), post-monsoon (e) and winter (f, g) seasons under stable conditions. The left panels (a, c, f) correspond to moderate wind conditions; the right panels (b, d, e, g) represent low wind conditions. The red line represents the ratio of best-fit curve obtained for respective seasons and wind speed classes.

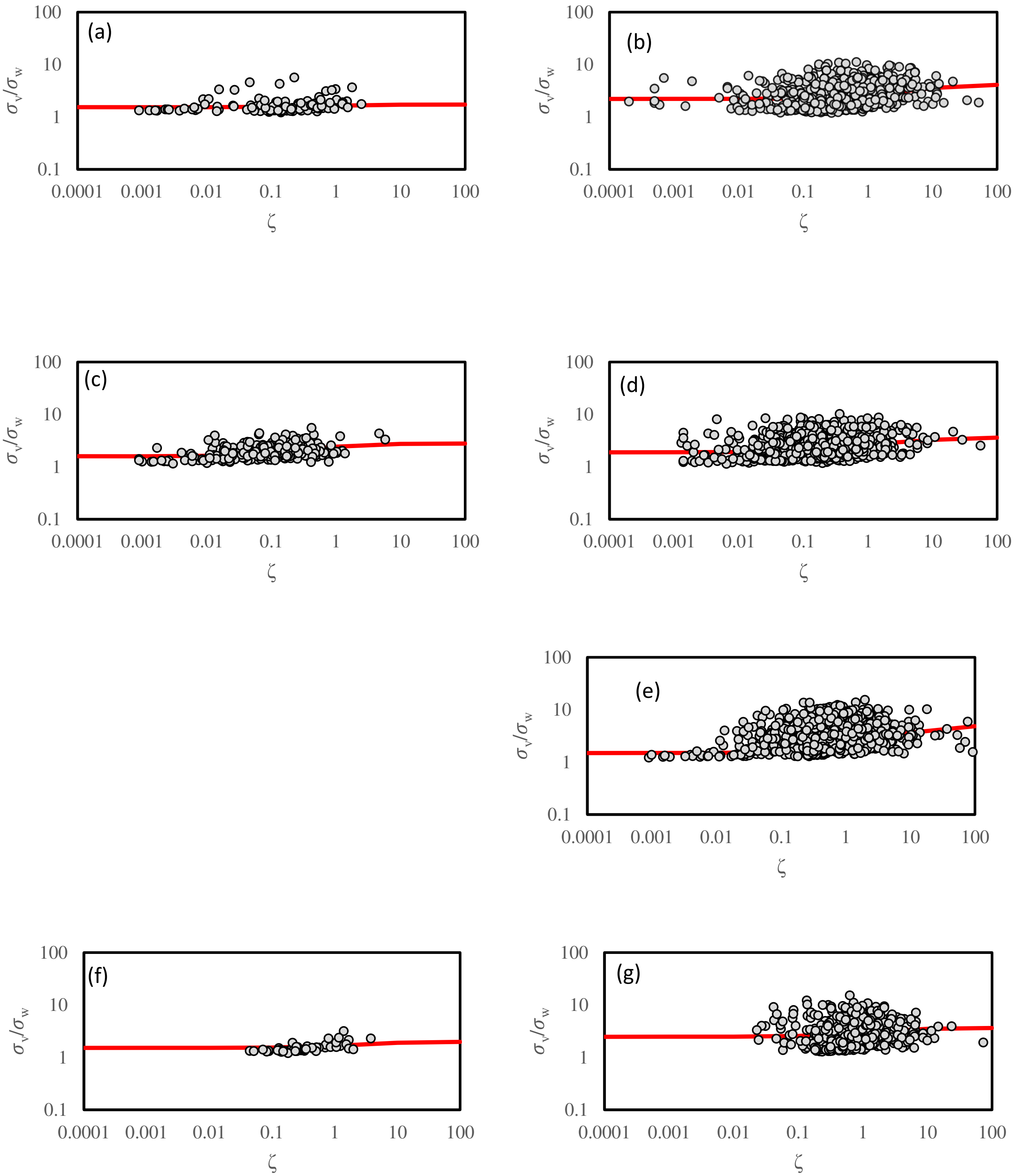

Fig. 15 Similar to Fig. 14, variation of $\varphi_v/\varphi_w = \sigma_v/\sigma_w$ with ζ for pre-monsoon (a, b), monsoon (c, d), post-monsoon (e) and winter (f, g) seasons under stable conditions. The left panels (a, c, f) correspond to moderate wind conditions; the right panels (b, d, e, g) represent low wind conditions. The red line represents the ratio of best-fit curve obtained for respective seasons and wind speed classes.

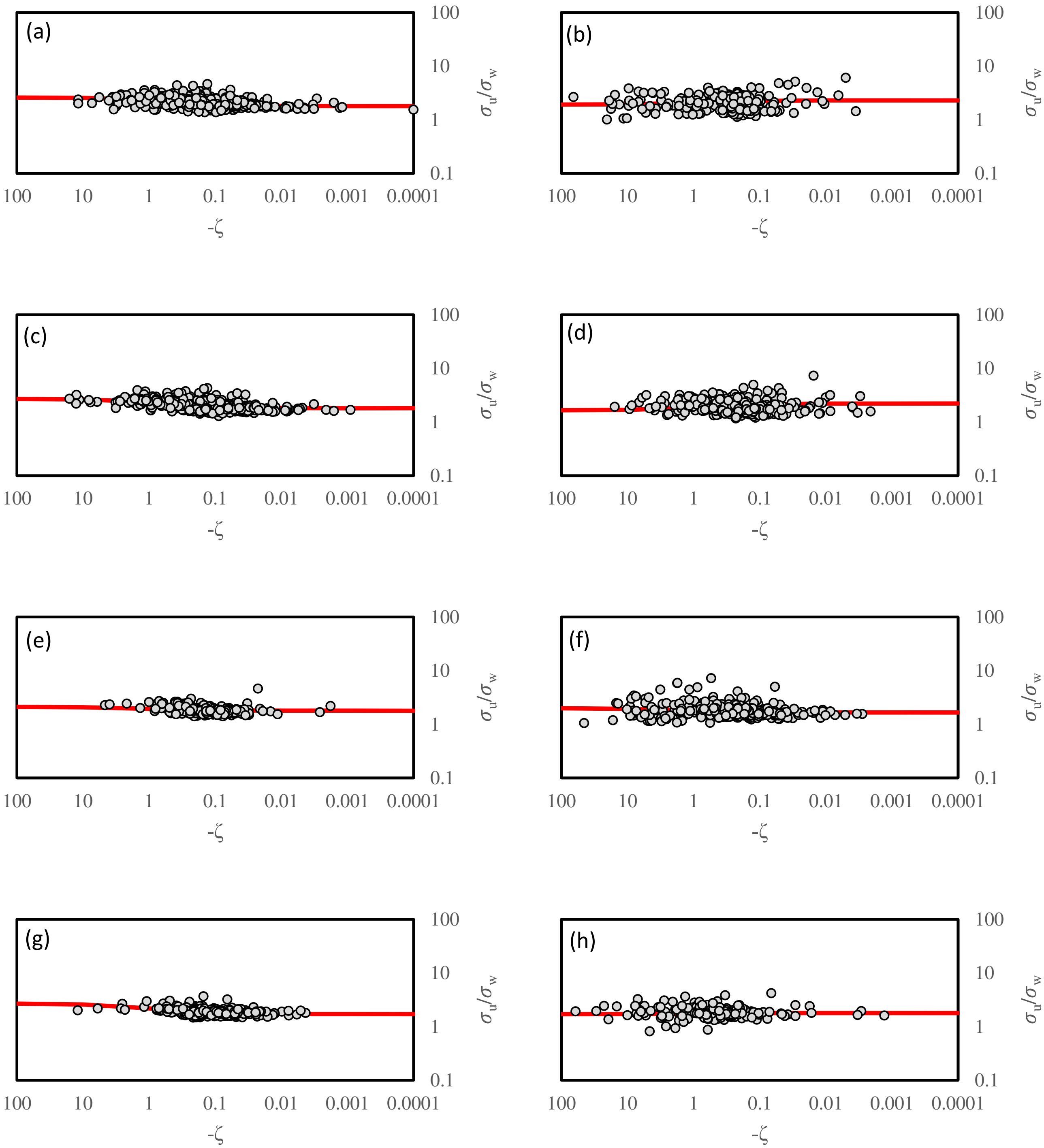

Fig. 16 Variation of $\varphi_u/\varphi_w = \sigma_u/\sigma_w$ with ζ for pre-monsoon (a, b), monsoon (c, d), post-monsoon (e) and winter (f, g) seasons under unstable conditions. The left panels (a, c, e, g) correspond to moderate wind conditions; the right panels (b, d, f, h) represent low wind conditions. The red line represents the ratio of best-fit curve obtained for respective seasons and wind speed classes.

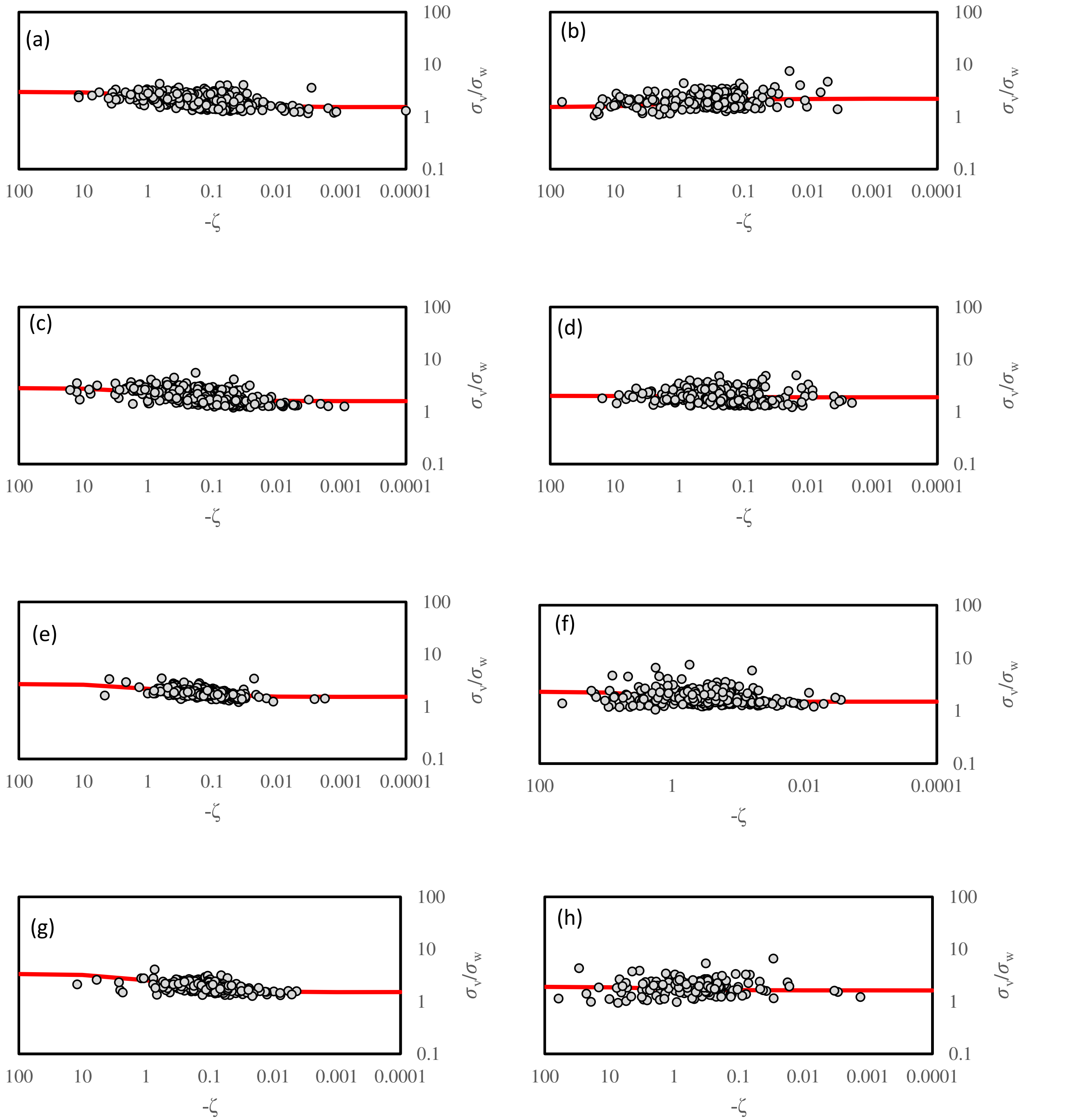

Fig. 17 Similar to Fig. 16, variation of $\varphi_v/\varphi_w = \sigma_v/\sigma_w$ with ζ for pre-monsoon (a, b), monsoon (c, d), post-monsoon (e, f) and winter (g, h) seasons under unstable conditions. The left panels (a, c, e, g) correspond to moderate wind conditions; the right panels (b, d, f, h) represent low wind conditions. The red line represents the ratio of best-fit curve obtained for respective seasons and wind speed classes.

Table 1: Quantitative description of data in each of the seasons under the different stability and wind speed regimes.

	Stable		Unstable		Transition		Daytime Stable		Nighttime Unstable	
Season	Low	Moderate	Low	Moderate	Low	Moderate	Low	Moderate	Low	Moderate
Pre-monsoon	660	114	232	568	103	64	20	11	144	22
Monsoon	676	255	356	551	124	88	26	40	250	60
Post-monsoon	860	4	400	361	172	8	124	14	156	1
Winter	437	51	160	301	86	16	33	11	80	1

Table 2: Table shows the empirical coefficients appearing in the expression (Eq. 5) in each of the seasons under the different stability and wind regimes. NA: no sufficient data points for estimating the coefficients.

	Season	**Stable**				**Unstable**			
		Low		**Moderate**		**Low**		**Moderate**	
		a	*b*	*a*	*b*	*a*	*b*	*a*	*b*
$\frac{\sigma_u}{u_*}$	Pre-monsoon	2.54	1.66	2.37	3.851	2.54	-1.01	2.37	-4.04
	Monsoon	2.48	3.32	2.50	7.60	2.48	-1.0	2.50	-3.50
	Post-monsoon	2.24	4.05	NA	NA	2.24	-0.88	2.43	-1.31
	Winter	2.41	2.04	2.30	1.13	2.41	-0.52	2.30	-2.35
$\frac{\sigma_v}{u_*}$	Pre-monsoon	2.45	0.84	2.03	1.78	2.45	-0.58	2.03	-9.89
	Monsoon	2.12	3.87	2.20	7.65	2.12	-2.89	2.20	-5.95
	Post-monsoon	2.01	2.13	NA	NA	2.01	-1.87	2.10	-4.26
	Winter	2.20	1.64	2.05	0.72	2.20	-0.97	2.05	-6.60
$\frac{\sigma_w}{u_*}$	Pre-monsoon	1.11	0.12	1.32	1.26	1.11	-1.73	1.32	-1.32
	Monsoon	1.12	0.81	1.38	1.41	1.12	-2.41	1.38	-1.05
	Post-monsoon	1.35	0.01	NA	NA	1.35	-0.51	1.36	-0.78
	Winter	0.9	0.5	1.35	0.32	1.25	-0.60	1.35	-0.59

Table 3: Statistical analysis of wind-velocity fluctuation standard deviations for different seasons, calculated using Eq. (5) and empirical coefficients derived using data from Pre-monsoon season (Table 2) for moderate wind conditions.

		Scheme	FB	NMSE	r
Stable	σ_u	Pre-monsoon	0.044	0.088	0.810
		Monsoon	-0.092	0.093	0.788
		Post-monsoon	NA	NA	NA
		Winter	0.161	0.118	0.821
	σ_v	Pre-monsoon	0.047	0.092	0.824
		Monsoon	-0.180	0.124	0.777
		Post-monsoon	NA	NA	NA
		Winter	0.079	0.098	0.830
	σ_w	Pre-monsoon	0.026	0.026	0.952
		Monsoon	-0.025	0.026	0.951
		Post-monsoon	NA	NA	NA
		Winter	0.044	0.028	0.955
Unstable	σ_u	Pre-monsoon	-0.012	0.032	0.784
		Monsoon	-0.049	0.036	0.782
		Post-monsoon	0.053	0.043	0.767
		Winter	0.277	0.040	0.776
	σ_v	Pre-monsoon	0.033	0.037	0.798
		Monsoon	0.034	0.038	0.791
		Post-monsoon	0.122	0.057	0.783
		Winter	0.089	0.047	0.793
	σ_w	Pre-monsoon	-0.053	0.015	0.942
		Monsoon	-0.086	0.022	0.941
		Post-monsoon	-0.060	0.018	0.940
		Winter	-0.044	0.017	0.940

Table 4: Statistical analysis of wind-velocity fluctuation standard deviations for different seasons, calculated using Eq. (5) and empirical coefficients derived using data from Pre-monsoon season (Table 2) for low wind conditions.

		Scheme	**FB**	**NMSE**	**r**
Stable	σ_u	Pre-monsoon	0.065	0.130	0.765
		Monsoon	-0.014	0.126	0.744
		Post-monsoon	0.052	0.139	0.734
		Winter	0.091	0.139	0.761
	σ_v	Pre-monsoon	0.052	0.151	0.735
		Monsoon	-0.054	0.161	0.684
		Post-monsoon	0.097	0.174	0.712
		Winter	0.042	0.156	0.724
	σ_w	Pre-monsoon	-0.010	0.163	0.791
		Monsoon	-0.107	0.168	0.776
		Post-monsoon	-0.185	0.199	0.793
		Winter	-0.185	0.199	0.793
Unstable	σ_u	Pre-monsoon	0.0005	0.091	0.748
		Monsoon	0.025	0.094	0.748
		Post-monsoon	0.137	0.124	0.747
		Winter	0.099	0.112	0.741
	σ_v	Pre-monsoon	0.034	0.071	0.822
		Monsoon	0.053	0.080	0.823
		Post-monsoon	0.164	0.115	0.827
		Winter	0.141	0.100	0.826
	σ_w	Pre-monsoon	0.013	0.025	0.889
		Monsoon	-0.040	0.025	0.889
		Post-monsoon	-0.083	0.048	0.876
		Winter	-0.093	0.048	0.878